Graphical Abstract

- Modelling habitat loss and fragmentation threats to mammal diversity across 804 ecoregions

- Considering distribution, habitat use, and dispersal distance of 4,179 non-volant mammal species

- Average of 10 predicted regional extinctions due to habitat loss and fragmentation

- Habitat fragmentation predicted to cause on average 10% of the species loss (but up to 90%)

Species loss

0 20 40 60 80

1   # Habitat fragmentation amplifies threats from habitat loss to

2   # mammal diversity across the world's terrestrial ecoregions

3   Koen JJ Kuipers[1,2*], Jelle P Hilbers[2], John Garcia-Ulloa[3], Bente J Graae[4], Roel May[5],

4   Francesca Verones[1], Mark AJ Huijbregts[2], Aafke M Schipper[2,6].

5   [1] Industrial Ecology Programme, Department of Energy and Process Engineering, NTNU, 7034 Trondheim, Norway

6   [2] Department of Environmental Science, Radboud University, 6526 AJ Nijmegen, the Netherlands

7   [3] Institute of Terrestrial Ecosystems, Department of Environmental Systems Science, ETH, 8092 Zürich, Switzerland

8   [4] Department of Biology, NTNU, 7491 Trondheim, Norway

9   [5] Department of Terrestrial Ecology, Norwegian Institute for Nature Research (NINA), 7485 Trondheim, Norway

10   [6] PBL Netherlands Environmental Assessment Agency, 2594 AV the Hague, the Netherlands

11   [*] Lead contact and correspondence: koen.kuipers@ru.nl

12   **Summary**

13   Global biodiversity is increasingly threatened by anthropogenic environmental change. At

14   present, 25% of comprehensively assessed species are threatened with extinction. While

15   there is mounting evidence that habitat loss is a key threat to biodiversity, global assessments

16   typically ignore additional threats from habitat fragmentation. Here, we present a new

17   species-area model that integrates habitat size and habitat connectivity, accounting for

18   species habitat preference, patch size, inter-patch distances, landscape matrix permeability

19   and species' dispersal capacity. We applied the model to predict the combined threat from

20   habitat loss and fragmentation to non-volant mammal species richness in 804 of the world's

21   terrestrial ecoregions. We predict that on average across the ecoregions, 10 mammal species

22   are committed to extinction due to habitat loss and fragmentation combined (range 0-86). On

23   average, 9% of the predicted species loss is due to fragmentation (range 0-90%). Considering

24   bot habitat loss and fragmentation, our model can be used for large-scale explorative

25   assessments to inform and evaluate strategies for minimising biodiversity loss due to the

26   expansion of human land use and for optimizing habitat conservation and restoration.

27   **Keywords**

28   Biodiversity, habitat connectivity, habitat conversion and fragmentation, land use, Mammalia,

29   species extinctions, species-area relationship.

Introduction

Due to the increasing human pressure on the natural environment, current species extinction rates are significantly higher than background rates, suggesting that we have entered a sixth mass extinction event [1,2]. At present 25% of the species comprehensively assessed by the International Union for the Conservation of Nature (IUCN) are threatened with extinction [1].

Habitat conversion has been identified as the predominant threat to biodiversity [1,3]. Time series of satellite observations reveal a rapid expansion of human land use at the cost of natural land cover [4–6]. Currently, over 77% of the terrestrial land cover has been affected by human activity [5], severely reducing the intactness of natural habitat [7,8], and scenario projections point at imminent further habitat conversion [9].

Global effects of habitat loss on biodiversity have been assessed in various recent studies, for example by synthesising local field observations [10], applying habitat suitability models [11,12], or by using species-area relationships (SARs) [13]. These assessments, however, generally ignore potential additional effects of habitat fragmentation, which may exacerbate biodiversity loss because populations in smaller and more isolated fragments are typically less viable [14,15]. As measures to combat habitat loss and fragmentation may differ [16], methods to estimate relative and combined effects of habitat loss and fragmentation globally are imperative to inform strategies to halt or reverse global biodiversity loss. This, in turn, is particularly relevant against the background of the upcoming post-2020 Global Biodiversity Framework [17].

Assessing effects of habitat loss and fragmentation on species diversity is complex, mainly due to variability in species' responses [18]. Fragmentation effects on species diversity are commonly studied via regression analyses relating empirical data on species diversity to habitat fragmentation variables (e.g., [14,19–21]). These empirical relationships can be combined with global land use maps to estimate global effects of fragmentation on local species diversity (e.g., [22]). Global estimates of assemblage-level responses to habitat loss and fragmentation can complement local, species-specific assessments to underpin large-scale strategies to combat negative biodiversity trends [1].

SAR models are commonly used to obtain global estimates of the threats from habitat loss to regional species diversity, generating estimates of imminent and longer-term future

59 extinctions of species that cannot persist given the size of the remaining habitat [1,13]. Although

60 SAR models are continuously being refined [23,24], they generally ignore connectivity between

61 habitat fragments [13,25]. Recently, Garcia-Ulloa et al. [26] proposed to combine species-area

62 models with the equivalent connected area (ECA) concept [27]. The ECA is a measure of area

63 weighted by its connectivity based on habitat fragment sizes and the probability of species'

64 dispersal between the fragments. The probability of dispersal is derived from the distance

65 between the fragments, permeability of the intermediate landscape matrix, and species'

66 dispersal capacity [28]. The ECA equals the total habitat area if all fragments are fully

67 connected, while it approaches the size of the largest single fragment if the fragments

68 become increasingly isolated.

69 Here, we present and apply a new SAR model that incorporates the ECA into the countryside

70 SAR (c-SAR) [23]. This integrated model, from hereon called the species-habitat relationship

71 (SHR), allows to systematically evaluate and compare threats from habitat loss and

72 fragmentation as it accounts for both habitat suitability (via the c-SAR model) and habitat

73 connectivity (via the ECA concept). By incorporating the ECA concept, the SHR considers

74 various relevant aspects of habitat fragmentation, including patch size, connectivity, and

75 matrix quality. Other fragmentation aspects, such as edge effects, are however not captured.

76 We applied the SHR model to evaluate threats from habitat loss and fragmentation on non-

77 volant mammal species diversity across the world's ecoregions ecoregions. We find that

78 threats from habitat loss are generally dominant over fragmentation threats, but that

79 fragmentation has a significant contribution and may even dominate the combined threat in

80 ecoregions characterised by severely fragmented habitats. Hence, considering habitat

81 fragmentation is relevant in global biodiversity assessments and for optimising area-based

82 conservation strategies.

83 **Results**

84 ***Threats from habitat loss and fragmentation combined***

85 The current global loss and fragmentation of natural habitat (as based on a land-use map for

86 2015; Fig. S1) corresponds with an average predicted loss of 10 mammal species across the

87 ecoregions (range = 0-86 species), equal to a relative loss of 11% on average (range = 0-

88 85%) (Fig. 1). In 578 of the 804 ecoregions (72%), at least one mammal species was

89   predicted to become regionally extinct. Predicted species loss was highest in the Yunnan

90   Plateau subtropical evergreen forests (species loss = 86), Sichuan Basin evergreen broadleaf

91   forests (species loss = 78), and Magdalena Valley dry forests (species loss = 77) ecoregions.

92   Relative species loss was predicted to be highest in Patía Valley dry forests (relative loss =

93   0.85), Magdalena Valley dry forests (relative loss = 0.75), and Cauca Valley dry forests

94   (relative loss = 0.73) ecoregions (see Data S2 for a complete overview of ecoregion-specific

95   results). Palearctic, Afrotropic, and Indomalayan ecoregions were predicted to be the most

96   affected and Oceanic and Australasian ecoregions the least, in terms of both absolute and

97   relative numbers of predicted extinctions. The similarity in the global patterns of absolute and

98   relative predicted species losses (Fig. S2) indicates that absolute species loss is determined

99   by the extent of land conversion and fragmentation rather than inherent differences in species

100   richness among the ecoregions.

101   *Contribution of habitat fragmentation*

102   The threats from habitat loss were generally dominant over the threats from fragmentation

103   (Fig. 2). On average across the ecoregions, habitat loss corresponded with a predicted loss of

104   nine species (range = 0-78), while fragmentation accounted for one additional extinction

105   (range = 0-18) and 9% of the combined threat. In 75 ecoregions (9%), fragmentation was

106   predicted to account for ≥25% of the combined threat and in 11 ecoregions (1%),

107   fragmentation threats contributed ≥50% (e.g., in the Guianan Piedmont and lowland moist

108   forests, Australian Alps montane grasslands, and Sulawesi lowland rain forests ecoregions;

109   Data S2). In 321 ecoregions (40%), fragmentation was predicted to cause at least one

110   additional mammal extinction. We further found a positive correlation between habitat loss

111   and fragmentation threats (Fig. 3), reflecting that more habitat conversion generally brings

112   about more fragmentation.

113   *Comparison with IUCN Red List*

114   Our average estimate of 10 predicted ecoregion-level extinctions (11%) is similar to the

115   estimate of the IUCN Red List [29], which reports on average eight species as extinct or

116   endangered and threatened by land use, corresponding to an average of 10% of the

117   ecoregional species pool. Further, we found a Spearman's rank correlation coefficient (ρ) of

118 0.49 between the numbers of extinct and endangered species predicted by our model and

119 estimated by the IUCN (Fig. 4).

120 Our assessment of fragmentation impacts provides a conservative estimate as we based our

121 calculations on species' maximum natal dispersal distance. Using the median natal dispersal

122 distance instead, we found on average two predicted extinctions (range = 0-19) due to

123 fragmentation instead of one (for details see the supplemental methods and Fig. S3). The

124 total number of predicted extinctions was similar (10 species in both dispersal scenarios, and

125 ranges of 0-86 and 0-88 in the maximum and median natal dispersal distance scenarios,

126 respectively), but the average contribution of fragmentation effects increased from 9% to 13%

127 (Fig. S4). Using the median rather than the maximum natal dispersal distance did not affect

128 the correlation between predicted and observed numbers of extinct and endangered species

129 (Spearman's ρ = 0.49; Fig. S5) or the relationship between predicted habitat conversion and

130 fragmentation effects (Fig. S2).

131 *Sensitivity analysis*

132 To assess the sensitivity of our model results to uncertainty in the slope of the SHR, we

133 performed additional calculations based on the 90% confidence intervals (CI) of the slope

134 values of the SHR, i.e. the species-area accumulation rates (Table S1). Changes in slope

135 values did not affect the predicted contribution of fragmentation effects, which remained on

136 average 9-10% (range = 0-90%; Table S2). The correlation between predicted and

137 documented numbers of extinct and endangered species also hardly changed by using

138 different slopes values (ρ = 0.43-0.51; Fig. S5). Global average predicted species loss,

139 however, changed by ±4 species (corresponding to ±4%) when adopting lower or upper 90%

140 CI slope values (with higher slope values resulting in higher predicted species loss; Table

141 S2).

142 As we applied the SHR to a global land-use map aggregated to a 1 km resolution (30"), our

143 assessment omits habitat patches smaller than 0.5 km^2 that could act as stepping stones and

144 thus improve habitat connectivity. To test the sensitivity of our results to the spatial resolution

145 of the land-use map, we applied the SHR at 300 m, 1 km, and 3 km resolutions for four small

146 ecoregions across different realms that are disproportionally affected by fragmentation. We

147 found that the average contribution of fragmentation effects increased from 4% at a low

148 resolution (3 km) to 8% at a high resolution (300 m; Table S3).

Discussion

150 Habitat loss is considered the main threat to biodiversity globally. Nevertheless, effects of

151 fragmentation are typically ignored in global biodiversity assessments, leading to a potential

152 underestimation of extinction risks. Here, we proposed and applied a method to estimate the

153 relative and combined threats from habitat loss and fragmentation to the diversity of non-

154 volant mammal species across the world's terrestrial ecoregions. Our results suggest that the

155 threats from habitat loss are generally dominant. This finding was independent of the

156 assumptions made with regard to species' dispersal capacity and slopes of the SHR (e.g.,

157 Figs S3-S5). Yet, we predicted that fragmentation threats are not negligible. Hence, land use

158 impact assessments that ignore additional fragmentation effects may systematically

159 underestimate species loss. Our ecoregion-level predictions indicate that the threats are

160 underestimated by about 10% on average, but the underestimation can be up to 90% in

161 highly fragmented ecoregions. In the Madagascar subhumid forests and the Sulawesi lowland

162 rain forests, for example, the predicted threats from fragmentation constitute more than half of

163 the total threats from habitat change, reflecting a highly fragmented remaining forest cover.

164 Divergent species responses to fragmentation may have contributed to the ongoing debate on

165 the relative significance of threats from habitat conversion and fragmentation [30–32]. We

166 estimated assemblage-level threats from habitat conversion and fragmentation across the

167 globe using a species-area model that consistently accounts for both the suitability and

168 connectivity of habitat. Turning off the threats of habitat fragmentation in our SHR model

169 enabled us to estimate the relative threats from habitat loss and fragmentation. Although we

170 found threats from habitat loss to be dominant over threats from habitat fragmentation,

171 predicted extinctions were higher in ecoregions with more fragmented habitat. This supports

172 conclusions from Haddad et al. [14] and Crooks et al. [15]. Furthermore, our results are in line with

173 local evidence from estimates of the impacts of forest fragmentation in Borneo, where

174 reduced functional connectivity for forest vertebrates imposed an additional 7% loss of

175 functional habitat [33].

176　For individual ecoregions, the total species loss predicted by the SHR may deviate from the

177　number of extinct and endangered species documented by the IUCN (Fig. 4). The IUCN data

178　are based on extinction risk assessments at the species level, whereas the SHR models net

179　changes in regional species richness (which may not reflect species-specific changes in a

180　specific location). Where possible, we parameterised the SHR based on the species pool

181　specific to each ecoregion (i.e., for land type suitability, matrix permeability, and body mass-

182　specific dispersal distance). Furthermore, we specified the species-area accumulation rates

183　(z) using mammal-specific values differentiated according to biome (Table S1; [34]). Yet, our

184　model does not cover all aspects that may influence projected species losses, including

185　species-specific dispersal behaviour, species' distributions within ecoregions, or differences in

186　species' accumulation rates among vegetation types. Additionally, we based our model

187　estimates on a relatively crude binary habitat classification scheme where a land type is either

188　suitable or unsuitable for a given species [29], whereas in reality species exhibit more subtle

189　differences in habitat use that need not align with simple land cover classes. Further, IUCN

190　threat levels are global in scope, which may cause a mismatch with the ecoregion-specific

191　SHR predictions (i.e., species could be more threatened in one ecoregion than in another).

192　Finally, the SHR considers effects of change in patch size, connectivity, and matrix quality,

193　and does therefore not incorporate other relevant aspects of fragmentation, such as edge

194　effects. Moreover, the SHR considers effects of habitat conversion only, and neglects threats

195　to species other than those caused by land use, such as overexploitation, pollution, or climate

196　change. Species covered by the IUCN can be endangered due to a variety of human

197　stressors in addition to habitat conversion [29]. Despite the deviations at ecoregion level,

198　however, we found a Spearman's rank correlation coefficient (ρ) between the SHR

199　predictions and IUCN data of 0.49 (Fig. 4) and a good match on average (10 vs 8 species

200　extinct or endangered). This suggests that our model can be used for large-scale exploratory

201　assessments of the threats from habitat loss and fragmentation on mammal species richness,

202　for example in comparative scenario projections [35,36], but it also highlights that predictions at

203　the ecoregional level are associated with uncertainty.

204　Yet, the non-negligible contribution of fragmentation to the predicted species loss emphasises

205　the need for more comprehensive assessments of land cover change effects on biodiversity.

206   Complementing mechanistic approaches assessing population-level responses [37], the SHR

207   provides an opportunity to systematically assess combined threats from habitat loss and

208   fragmentation on species richness across large extents, as it is relatively easily parametrised

209   for different species groups and spatial units by adapting the SHR species-accumulation

210   rates, land type suitabilities and dispersal capacities. Using the SHR in combination with land

211   use scenarios would allow for estimating the consequences of different land use 'futures',

212   including further conversion of natural habitat as well as restoration. This can inform and help

213   to evaluate strategies for minimising effects of expansion of human land use, support habitat

214   restoration programs, or contribute to the effective allocation and design of conservation and

215   protected areas in combination with prioritisation procedures [38]. Our comparative assessment

216   across three spatial resolutions indicates that predictions with the SHR model are preferably

217   made based on high-resolution land use maps. Coarse resolutions may aggregate small

218   fragmented patches to a larger single patch (similar to functionally connected patches).

219   Hence, application at coarse resolutions may underestimate fragmentation. This indicates the

220   importance of small habitat patches as stepping stones in the landscape [39].

221   Curtailing biodiversity loss rates requires acute and significant conservation efforts. As most

222   targets set within the Strategic Plan for Biodiversity 2011-2020 have not been reached, there

223   are major challenges in the ongoing negotiations towards a post-2020 Global Biodiversity

224   Framework [17]. Given that land use is a key driver of biodiversity loss and that feeding the

225   growing human population may further increase the demand for land, there is a key role for

226   strategies to minimise impacts of habitat conversion on biodiversity and ecosystems [40,41].

227   Combining the SHR with global land use projections would enable evaluating the effects of

228   both the amount and spatial configuration of habitat. In turn, this information can play a role in

229   designing comprehensive conservation strategies based on contrasting paradigms and

230   corresponding measures (e.g., sparing versus sharing; [42,43]). The ability to predict large-scale

231   landscape configuration effects on regional species diversity is a pivotal component towards

232   designing area-based conservation strategies for meeting internationally agreed targets for

233   halting or restoring biodiversity loss. These large-scale assessments should in turn be

234   complemented by an understanding of local and species-specific responses to habitat loss

235   and fragmentation, which do not necessarily correspond with the large-scale assemblage-

236 level patterns (e.g., [14,20,21,44,45]). Improved understanding of biodiversity change at global,

237 regional, and local scales is key for identifying comprehensive and targeted conservation

238 measures and meeting biodiversity targets [46].

239 **Experimental procedures**

240 *Resource availability*

241 *Lead contact*

242 Further information and requests for resources should be directed to and will be fulfilled by

243 the lead contact, Koen Kuipers (koen.kuipers@ru.nl).

244 *Materials availability*

245 The datasets with habitat affinity, matrix conductivity, and dispersal distance (Data S1), and

246 ecoregional habitat data (i.e., equivalent connected area, species richness, habitat suitability,

247 species-accumulation rates, and dispersal distances; Data S2) have been deposited to

248 Figshare under doi.org/10.6084/m9.figshare.16616650.v1.

249 *Data and code availability*

250 All original data used in this research are publicly available. Species distribution spatial data

251 and habitat documentation data are deposited by IUCN Red List of Threatened Species.

252 Mammal species body mass data are deposited on Figshare under

253 doi.org/10.6084/m9.figshare.c.3306933.v1. Ecoregion spatial data area deposited by WWF

254 under doi.org/10.1641/0006-3568(2001)051[0933:TEOTWA]2.0.CO;2. 2015 land-use and

255 land cover spatial data is deposited by the GLOBIO project under doi.org/10.1111/gcb.14848.

256 The European Space Agency (ESA) Climate Change Initiative (CCI) land cover (LC) data is

257 deposited by the ECA-CCI-LC and publicly available upon request at http://www.esa-

258 landcover-cci.org/?q=node/164. The potential natural vegetation data is deposited by the Oak

259 Ridge National Laboratory (ORNL) Distributed Active Archive Center (DAAC) under

260 doi:10.3334/ORNLDAAC/961.

261 Code treating the raw data to parametrise the SHR and generate results of this publication

262 (Code S1-3) are available in on Figshare under doi.org/10.6084/m9.figshare.16616650.v1.

263 ***Model description***

264 The species-habitat relationship (SHR) models the relationship between the number of

265 species committed to extinction and the suitability and spatial configuration of various land-

266 use and land cover types (hereafter referred to as land types). It is an integration of the

267 countryside SAR (c-SAR) [23] and the equivalent connected area (ECA) concept [27] such that

268 the area variable of the conventional c-SAR is replaced by the ECA [26]. The differential

269 suitability of various land types considered in the c-SAR can be considered equivalent to

270 matrix permeability, which in turn is a key parameter in the ECA. Thus, the integration of c-

271 SAR and ECA allows for consistent modelling of land type suitability and matrix permeability

272 across all ecoregions, considering that distinct land types host different species groups and

273 that some species may occur across several land types.

274 Similar to how the c-SAR can be used to estimate relative species loss (RSL) due to habitat

275 loss [13,25], the SHR can be used to estimate RSL due to both habitat conversion and

276 fragmentation (equation 1), as

277 (1) $\quad RSL = 1 - \left(\frac{\sum_i h_i \cdot ECA_i}{\sum_i h_i \cdot ECA_{i,ref}} \right)^z$

278 where h_i is the suitability of land type i, ECA_i is the ECA of land type i, $ECA_{i,ref}$ is the ECA of

279 land type i in the reference landscape (i.e., no human land use), and z is the slope (i.e.,

280 species accumulation rate) of the species-habitat curve. Absolute species loss can be

281 quantified by multiplying the RSL with the number of species in the reference state.

282 Land type suitabilities (h) are defined as the proportion of species occurring in land type i

283 relative to the total number of species in the region, raised to the power 1/z (equation 2) [13].

284 (2) $\quad h_i = \left(\frac{S_i}{S} \right)^{1/z}$

285 The *ECA* considers the spatial configuration of the landscape and the degree of

286 fragmentation as perceived by the species group occurring in land type i. The *ECA* is based

287 on the number and size (a) of individual habitat patches m and n of land type i and the

288 probability of dispersal (p) between each pair of patches m and n (equation 3).

289 (3) $\quad ECA_i = \left(\sum_{m,n} a_{i,m} \cdot a_{i,n} \cdot p_{i,mn} \right)^{0.5}$

290 The probability of dispersal (p) among patches of land type i is defined by the dispersal kernel

291 based on the least-cost distance (w) between habitat patches m and n and the dispersal

292 distance (α) of the species occurring in land type i [47] (equation 4).

293 (4) $\quad p_{i,mn} = e^{-w_{i,mn}/\alpha_i}$

294 The least-cost distance (w) is defined as the permeability-weighted length of the route that

295 results in the shortest distance between patch m and n [28] by multiplying the distance d

296 travelled through landscape matrix type k by the resistance (r) of the matrix type (equation 5)

297 [26]. Relatively permeable matrix types form so-called "stepping stones", improving the

298 connectivity of distant patches [28].

299 (5) $\quad w_{i,mn} = \sum_k d_{i,mn,k} \cdot r_{i,k}$

300 The permeability of the matrix separating the habitat patches of land type i is based on the

301 overlap of species between land type i and matrix type k (i.e., the number of species

302 occurring in both land type i and matrix type k; equation 6).

303 (6) $\quad r_{i,k} = 1 - \frac{s_{i,k}}{s_i}$

304 If species that occur in land type i all occur in matrix type k, the permeability equals 1 (i.e., a

305 resistance of 0), meaning that this matrix type can be crossed without any cost. Hence, the

306 connectivity of the landscape depends on the species overlap between the land types:

307 habitats in regions with large overlap of species communities between land types are more

308 connected than habitats with distinct communities.

309 ***Model parametrisation***

310 We model the threats from land cover change to species richness at the level of ecoregions,

311 i.e., distinct biogeographical units that can be considered relatively homogeneous in their

312 vegetation and species pool [48]. We cover 804 of the 825 terrestrial ecoregions based on

313 available land type and species data. We retrieved the spatial configuration of the land types

314 in each ecoregion, needed to quantify patch area sizes (a) and the spatial configuration of the

315 landscape, from a high-resolution land-use map for 2015 [22]. To reduce computation time, we

316 resampled the land-use map from 10" (300 m near the equator) to 30" (900 m near the

317 equator) based on the mode (i.e., majority rule) and aggregated the original land type classes

318 into eight major land types (Table S4). Four land types are anthropogenic (urban, cropland,

319 pasture, and forestry) and four are natural (forests, grasslands, deserts, and rock and ice).

320 We replaced the original class "light use pasture" by the land cover in the underlying

321 European Space Agency Climate Change Initiative land cover [49], as this class indicates

322 natural habitat that is used mainly for extensive grazing [50]. To establish a baseline natural

323 land cover map, we replaced all anthropogenic land cover by natural land cover as defined by

324 the ISLCSP II Potential Natural Vegetation Cover map [51,52]. We retrieved biome-specific

325 mammal species-area accumulation rates from Kehoe et al. [34], ranging from 0.14 (boreal

326 forest ecoregions, n = 28) to 0.49 (tropical and subtropical coniferous forest ecoregions, n =

327 16) (Table S1).

328 We derived land type suitability (h) and matrix resistance values (r) per ecoregion from

329 species' occurrence ranges and species habitat affinities as documented by IUCN of 4,179

330 non-volant mammal species, representing ~90% of all known extant non-volant mammals

331 [29,53]. We have excluded flying mammals (bats) because of uncertain and divergent dispersal

332 behaviour in response to fragmentation compared to non-volant mammals [21]. For deriving

333 land type suitability (h) and matrix resistance (r) values, we first obtained the number of non-

334 volant mammal species (S) per ecoregion based on the overlap of IUCN species range maps

335 (n = 4,179) with the ecoregions [29]. We then defined the land type suitability of each land type i

336 in each ecoregion based on the number of species with affinity to that land use type relative to

337 the total number of species in the ecoregion [29]. The subset of species of land type i that also

338 occur in matrix type k was obtained correspondingly.

339 We define dispersal capacities (α) as the median of the maximum natal dispersal distance of

340 the species specific to each ecoregion and land type i. Using the maximum natal dispersal

341 distance is in line with metapopulation theory [54], as it gives an indication of the possibility of

342 species to reach isolated habitat fragments [54]. We retrieved species-specific maximum

343 dispersal distances using allometric relationships between mammal body mass (b) and home

344 range, and home range and maximum natal dispersal capacity, differentiated according to

345 trophic guild [55,56]. For carnivorous mammals, the species-specific maximum dispersal

346 distance is estimated by $\alpha = 40\sqrt{380b^{1.13}}$; for non-carnivorous mammals, the species-specific

347   maximum dispersal distance is estimated by $\alpha = 40\sqrt{54b}$ (where dispersal distance and body

348   mass are in meters and grams, respectively). We extracted species-specific body mass (b)

349   and trophic guild data from the EltonTraits 1.0 database [57].

350   The slope of the SHR (z) indicates the rate at which species richness increases with

351   equivalent connected area. Such species-area slopes are commonly assumed to range

352   between 0.2 and 0.3, depending on geographical location and environmental conditions

353   [13,23,25]. We retrieved mammal- and biome-specific z values from Kehoe et al. [34], who

354   assessed terrestrial mammal species richness in plots of increasing size based on species'

355   range maps.

356   We assessed threats from habitat loss only by ignoring changes in connectivity after habitat

357   conversion (i.e., assuming human-modified land cover to be equally permeably as the original

358   land cover). We assessed the additional threats from fragmentation as the difference between

359   the predicted species loss caused by habitat conversion and fragmentation combined and the

360   predicted species loss caused by habitat conversion only.

361   We validated the predicted threats from habitat conversion and fragmentation per ecoregion

362   against the number of extinct and endangered species as documented by the IUCN [29], similar

363   to previous studies that validated SAR-based models of species loss (e.g., [35,58,59]). We

364   identified the number of non-flying mammal species per ecoregion, listed as "extinct", "extinct

365   in wild", "critically endangered", "endangered", or "vulnerable" and threatened by at least one

366   land-use category (from the categories "commercial development", "agriculture", "pasture",

367   and "plantations") (n = 795) and calculated the proportion relative to the total number of non-

368   volant mammals (n = 3,659) in the region (excluding "data deficient" species). Furthermore,

369   we excluded species listed as threatened due to criteria A1-4de only (n = 17) because these

370   species are threatened due to overexploitation or exotic alien species and would be listed as

371   threatened even if their habitat remains fully intact. We included both extinct and endangered

372   species, because SAR models estimate both materialised and projected extinctions [13]. We

373   then compared our estimates of relative and absolute species extirpations due to the

374   combined effects of habitat conversion and fragmentation with the relative and absolute

375   number of endangered species threatened with land use according to the IUCN.

376 ***Model simulations for sensitivity assessment***

377 We tested the sensitivity of the outcomes to key parameters by considering different

378 assumptions regarding dispersal capacities (α), species-area accumulation rates (*z*), and land

379 use map resolutions.

380 To assess the sensitivity of our outcomes to the dispersal distance parameter (α), we also

381 performed the calculations based on median rather than maximum natal dispersal distances,

382 resulting in lower species mobility and landscape connectivity. We obtained species-specific

383 median natal dispersal distances from corresponding relationships between body mass and

384 dispersal distance (via body mass-home range, and home range-dispersal distance

385 relationships), estimated as $\alpha = 7\sqrt{380b^{1.13}}$ for carnivorous mammals and $\alpha = 7\sqrt{54b}$ for non-

386 carnivorous mammals (where dispersal distance and body mass are in meters and grams,

387 respectively) [55].

388 We assessed the sensitivity of our results to changes in the slope (*z*) of the SHR by applying

389 lower and higher biome-specific *z*-values based on their 90% confidence intervals (capped

390 between 0 and 1; Table S1).

391 Finally, we assessed the effect of the resolution of the land use map. To that end, we applied

392 the SHR to habitat change in four selected small ecoregions across different realms that are

393 disproportionally affected by fragmentation (Table S3), using resolutions of 300 m (10"), 1 km

394 (30"), and 3 km (100").

399 **Author contributions**

400 Conceptualisation, K.J.J.K., J.P.H., J.C.U., B.J.G., R.M., F.V., M.A.J.H., and A.M.S.;

401 Methodology (approach, model, and parameter development), K.J.J.K., J.P.H., M.A.J.H., and

402 A.M.S.; Software (code preparation and application), K.J.J.K.; Formal analysis, K.J.J.K.;

403 Writing – original draft, K.J.J.K., M.A.J.H., and A.M.S.; Writing – review & editing, K.J.J.K.,

404 J.P.H., J.C.U., B.J.G., R.M., F.V., M.A.J.H., and A.S.

Declaration of interest

The authors declare no competing interests.

References

1. IPBES (2019). Global assessment report of the Intergovernmental Science-Policy Platform on Biodiversity and Ecosystem Services. E. S. Brondízio, J. Settele, S. Díaz, and H. T. Ngo, eds. (IPBES secretariat, Bonn, Germnay; 1144 pages, ISBN: 978-3-947851-20-1): https://ipbes.net/global-assessment.

2. Ceballos, G., Ehrlich, P.R., and Dirzo, R. (2017). Biological annihilation via the ongoing sixth mass extinction signaled by vertebrate population losses and declines. Proc. Natl. Acad. Sci., 6089–6096.

3. Maxwell, S.L., Fuller, R.A., Brooks, T.M., and Watson, J.E.M. (2016). Biodiversity: The ravages of guns, nets and bulldozers. Nature *536*, 143–145.

4. Potapov, P., Hansen, M.C., Laestadius, L., Turubanova, S., Yaroshenko, A., Thies, C., Smith, W., Zhuravleva, I., Komarova, A., Minnemeyer, S., et al. (2017). The last frontiers of wilderness: Tracking loss of intact forest landscapes from 2000 to 2013. Sci. Adv. *3*, 1–14.

5. Watson, J.E.M., Venter, O., Jasmine, L., Jones, K.R., Robinson, J.G., Possingham, H.P., and Allan, J.R. (2018). Protect the last of the wild. Nature *563*, 27–30.

6. Ellis, E.C. (2019). To Conserve Nature in the Anthropocene, Half Earth Is Not Nearly Enough. One Earth *1*, 163–167.

7. Beyer, H.L., Venter, O., Grantham, H.S., and Watson, J.E.M. (2020). Substantial losses in ecoregion intactness highlight urgency of globally coordinated action. Conserv. Lett. *13*, e12692.

8. Williams, B.A., Venter, O., Allan, J.R., Atkinson, S.C., Rehbein, J.A., Ward, M., Di Marco, M., Grantham, H.S., Ervin, J., Goetz, S.J., et al. (2020). Change in Terrestrial Human Footprint Drives Continued Loss of Intact Ecosystems. One Earth *3*, 371–382.

9. Powers, R.P., and Jetz, W. (2019). Global habitat loss and extinction risk of terrestrial vertebrates under future land-use-change scenarios. Nat. Clim. Chang. *9*, 323–329.

10. Newbold, T., Hudson, L.N., Hill, S.L., Contu, S., Lysenko, I., Senior, R. a, Börger, L., Bennett, D.J., Choimes, A., Collen, B., et al. (2015). Global effects of land use on local

435   terrestrial biodiversity. Nature *520*, 45–50.

436 11. Visconti, P., Bakkenes, M., Baisero, D., Brooks, T., Butchart, S.H.M., Joppa, L.,

437   Alkemade, R., Di Marco, M., Santini, L., Hoffmann, M., et al. (2014). Projecting Global

438   Biodiversity Indicators under Future Development Scenarios. Conserv. Lett. *9*, 5–13.

439 12. Baisero, D., Visconti, P., Pacifici, M., and Cimatti, M. (2020). Projected Global Loss of

440   Mammal Habitat Due to Land-Use and Climate Change Projected Global Loss of

441   Mammal Habitat Due to Land-Use and Climate Change. One Earth *2*, 578–585.

442 13. Martins, I.S., and Pereira, H.M. (2017). Improving extinction projections across scales

443   and habitats using the countryside species-area relationship. Nat. Sci. Reports *7*, 1–7.

444 14. Haddad, N.M., Brudvig, L. a., Clobert, J., Davies, K.F., Gonzalez, A., Holt, R.D.,

445   Lovejoy, T.E., Sexton, J.O., Austin, M.P., Collins, C.D., et al. (2015). Habitat

446   fragmentation and its lasting impact on Earth's ecosystems. Sci. Adv. *1*, 1–9.

447 15. Crooks, K.R., Burdett, C.L., Theobald, D.M., King, S.R.B., Di Marco, M., Rondinini, C.,

448   and Boitani, L. (2017). Quantification of habitat fragmentation reveals extinction risk in

449   terrestrial mammals. Proc. Natl. Acad. Sci. *114*, 7635–7640.

450 16. Wei, F., Swaisgood, R., Hu, Y., Nie, Y., Yan, L., Zhang, Z., Qi, D., and Zhu, L. (2015).

451   Progress in the ecology and conservation of giant pandas. Conserv. Biol. *29*, 1497–

452   1507.

453 17. Nature Editorial (2020). New biodiversity targets cannot afford to fail. Nature *578*, 337–

454   338.

455 18. Ewers, R.M., and Didham, R.K. (2005). Confounding factors in the detection of

456   species responses to habitat fragmentation. Biol. Rev. *81*, 117–142.

457 19. Martensen, A.C., Ribeiro, M.C., Banks-Leite, C., Prado, P.I., and Metzger, J.P. (2012).

458   Associations of Forest Cover, Fragment Area, and Connectivity with Neotropical

459   Understory Bird Species Richness and Abundance. Conserv. Biol. *26*, 1100–1111.

460 20. Keinath, D.A., Doak, D.F., Hodges, K.E., Prugh, L.R., Fagan, W., Sekercioglu, C.H.,

461   Buchart, S.H.M., and Kauffman, M. (2017). A global analysis of traits predicting

462   species sensitivity to habitat fragmentation. Glob. Ecol. Biogeogr. *26*, 115–127.

463 21. Lino, A., Fonseca, C., Rojas, D., Fischer, E., and Ramos Pereira, M.J. (2019). A meta-

464   analysis of the effects of habitat loss and fragmentation on genetic diversity in

465 mammals. Mamm. Biol. *94*, 69–76.

466 22. Schipper, A.M., Hilbers, J.P., Meijer, J., Antão, J., Benítez-López, A., de Jonge, M.,

467 Leemans, L., Scheper, E., Alkemade, R., Doelman, J., et al. (2020). Projecting

468 terrestrial biodiversity intactness with GLOBIO 4. Glob. Chang. Biol. *26*, 760–771.

469 23. Pereira, H.M., and Daily, G.C. (2006). Modeling biodiversity dynamics in countryside

470 landscapes. Ecology *87*, 1877–1885.

471 24. Koh, L.P., and Ghazoul, J. (2010). A matrix-calibrated species-area model for

472 predicting biodiversity losses due to land-use change. Conserv. Biol. *24*, 994–1001.

473 25. Marques, A., Martins, I.S., Kastner, T., Plutzar, C., Theurl, M.C., Eisenmenger, N.,

474 Huijbregts, M.A.J., Wood, R., Stadler, K., Bruckner, M., et al. (2019). Increasing

475 impacts of land use on biodiversity and carbon sequestration driven by population and

476 economic growth. Nat. Ecol. Evol. *3*, 628–637.

477 26. Garcia-Ulloa, J., Giam, X., Rondinini, C., Saura, S., and Koh, L.P. (2016).

478 Incorporating graph theory into species-area modelling of land use change impacts. In

479 the doctoral thesis of John Garcia-Ulloa: Improving Conservation Perspectives of

480 Land-Use Change Policies in the Tropics (Department of Environmental Systems

481 Science, ETH Zürich), pp. 19–47.

482 27. Saura, S., Estreguil, C., Mouton, C., and Rodríguez-Freire, M. (2011). Network

483 analysis to assess landscape connectivity trends: Application to European forests

484 (1990-2000). Ecol. Indic. *11*, 407–416.

485 28. Saura, S., and Pascual-Hortal, L. (2007). A new habitat availability index to integrate

486 connectivity in landscape conservation planning: Comparison with existing indices and

487 application to a case study. Landsc. Urban Plan. *83*, 91–103.

488 29. IUCN (2020). The IUCN Red List of Threatened Species. Version 2020-2.

489 http://www.iucnredlist.org.

490 30. Fahrig, L., Arroyo-Rodríguez, V., Bennett, J.R., Boucher-Lalonde, V., Cazetta, E.,

491 Currie, D.J., Eigenbrod, F., Ford, A.T., Harrison, S.P., Watling, J.I., et al. (2019). Is

492 habitat fragmentation bad for biodiversity? Biol. Conserv. *230*, 179–186.

493 31. Fletcher, R.J., Didham, R.K., Banks-Leite, C., Barlow, J., Ewers, R.M., Rosindell, J.,

494 Holt, R.D., Gonzalez, A., Pardini, R., Damschen, E.I., et al. (2018). Is habitat

495   fragmentation good for biodiversity? Biol. Conserv. *226*, 9–15.

496   32.   Betts, M.G., Wolf, C., Pfeifer, M., Banks-Leite, C., Arroyo-Rodríguez, V., Ribeiro, D.B.,

497   Barlow, J., Eigenbrod, F., Faria, D., Fletcher Jr., R.J., et al. (2019). Extinction filters

498   mediate the global effects of habitat fragmentation on animals. Science (80-.). *366*,

499   1236–1239.

500   33.   Ocampo-Peñuela, Garcia-ulloa, J., Kornecki, I., Philipson, C.D., and Ghaozoul, J.

501   (2020). Impacts of four decades of forest loss on vertebrate functional habitat on

502   Borneo. Front. For. Glob. Chang. *3*, 1–13.

503   34.   Kehoe, L., Senf, C., Meyer, C., Gerstner, K., Kreft, H., and Kuemmerle, T. (2017).

504   Agriculture rivals biomes in predicting global species richness. Ecography (Cop.). *40*,

505   1118–1128.

506   35.   Wearn, O.R., Reuman, D.C., and Ewers, R.M. (2012). Extinction debt and windows of

507   conservation opportunity in the Brazilian Amazon. Science (80-.). *337*, 228–233.

508   36.   Di Marco, M., Harwood, T.D., Hoskins, A.J., Ware, C., Hill, S.L.L., and Ferrier, S.

509   (2019). Projecting impacts of global climate and land-use scenarios on plant

510   biodiversity using compositional-turnover modelling. Glob. Chang. Biol. *25*, 2763–

511   2778.

512   37.   Cosgrove, A.J., McWhorter, T.J., and Maron, M. (2018). Consequences of

513   impediments to animal movements at different scales: A conceptual framework and

514   review. Divers. Distrib. *24*, 448–459.

515   38.   Mokany, K., Ferrier, S., Harwood, T.D., Ware, C., Di Marco, M., Grantham, H.S.,

516   Venter, O., Hoskins, A.J., and Watson, J.E.M. (2020). Reconciling global priorities for

517   conserving biodiversity habitat. Proc. Natl. Acad. Sci. U. S. A. *117*, 9906–9911.

518   39.   Lindenmayer, D. (2019). Small patches make critical contributions to biodiversity

519   conservation. Proc. Natl. Acad. Sci. U. S. A. *116*, 717–719.

520   40.   Pouzols, F.M., Toivonen, T., Minin, E. Di, Kukkala, A.S., Kullberg, P., Kuustera, J.,

521   Lehtomaki, J., Tenkanen, H., Verburg, P.H., and Moilanen, A. (2014). Global protected

522   area expansion is compromised by projected land-use and parochialism. Nature *516*,

523   383–386.

524   41.   Pimm, S.L., Jenkins, C.N., and Li, B. V. (2018). How to protect half of earth to ensure

525   it protects sufficient biodiversity. Sci. Adv. *4*, 1–9.

526   42.   Kok, M., Meijer, J.R., Zeist, W.-J. van, Hilbers, J., Immovilli, M., Janse, J., Stehfest, E.,

527   Bakkenes, M., Tabeau, A., Schipper, A., et al. (2020). Assessing ambitious nature

528   conservation strategies within a 2 degree warmer and food-secure world. bioRxiv,

529   2020.08.04.236489.

530   43.   Phalan, B., Onial, M., Balmford, A., and Green, R.E. (2011). Reconciling food

531   production and biodiversity conservation: land sharing and land sparing compared.

532   Science (80-.). *333*, 1289–1291.

533   44.   Püttker, T., Bueno, A.A., dos Santos de Barros, C., Sommer, S., and Pardini, R.

534   (2013). Habitat specialization interacts with habitat amount to determine dispersal

535   success of rodents in fragmented landscapes. J. Mammal. *94*, 714–726.

536   45.   Estavillo, C., Pardini, R., and Da Rocha, P.L.B. (2013). Forest loss and the biodiversity

537   threshold: An evaluation considering species habitat requirements and the use of

538   matrix habitats. PLoS One *8*, 1–10.

539   46.   McGill, B.J., Dornelas, M., Gotelli, N.J., and Magurran, A.E. (2015). Fifteen forms of

540   biodiversity trend in the anthropocene. Trends Ecol. Evol. *30*, 104–113.

541   47.   Moilanen, A. (2004). SPOMSIM: Software for stochastic patch occupancy models of

542   metapopulation dynamics. Ecol. Modell. *179*, 533–550.

543   48.   Olson, D.M., Dinerstein, E., Wikramanayake, E.D., Burgess, N.D., Powell, G.V.N.,

544   Underwood, E.C., D'amico, J. a., Itoua, I., Strand, H.E., Morrison, J.C., et al. (2001).

545   Terrestrial Ecoregions of the World: A New Map of Life on Earth. Bioscience *51*, 933–

546   938.

547   49.   ESA (2017). Land Cover CCI Product, User Guide Version 2.0. 1–104.

548   http://maps.elie.ucl.ac.be/CCI/viewer/download/ESACCI-LC-Ph2-PUGv2_2.0.pdf.

549   50.   Alkemade, R., Reid, R.S., van den Berg, M., de Leeuw, J., and Jeuken, M. (2013).

550   Assessing the impacts of livestock production on biodiversity in rangeland

551   ecosystems. Proc. Natl. Acad. Sci. *110*, 20900–20905.

552   51.   Ramankutty, N., Foley, J.A., Hall, F., Gollatz, G., Meeson, B., Los, S., Brown de

553   Colstoun, E., and Landis, D. (2010). ISLSCP II Potential Natural Vegetation cover.

554   52.   Gallego-Zamorano, J., Benítez-López, A., Santini, L., Hilbers, J.P., Huijbregts, M.A.J.,

555   and Schipper, A.M. (2020). Combined effects of land use and hunting on distributions

556   of tropical mammals. Conserv. Biol., 1–10.

557 53. Burgin, C.J., Colella, J.P., Kahn, P.L., and Upham, N.S. (2018). How many species of

558   mammals are there? J. Mammal. *99*, 1–14.

559 54. Hanski, I., and Ovaskainen, O. (2000). The metapopulation capacity of a fragmented

560   landscape. Nature *404*, 755–758.

561 55. Bowman, J., Jaeger, J.A.G., and Fahrig, L. (2002). Dispersal distance of mammals is

562   proportional to home range size. Ecology *83*, 2049–2055.

563 56. Hilbers, J.P., Schipper, A.M., Hendriks, A.J., Verones, F., Pereira, H.M., and

564   Huijbregts, M.A.J. (2016). An allometric approach to quantify the extinction

565   vulnerability of birds and mammals. Ecology *97*, 615–626.

566 57. Wilman, H., Belmaker, J., Simpson, J., de la Rosa, C., Rivadeneira, M.M., and Jetz,

567   W. (2014). EltonTraits 1.0: Species-level foraging attributes of the world's birds and

568   mammals. Ecology *95*, 2027.

569 58. Pereira, H.M., Ziv, G., and Miranda, M. (2014). Countryside species-area relationship

570   as a valid alternative to the matrix-calibrated species-area model. Conserv. Biol. *28*,

571   874–876.

572 59. Chaudhary, A., and Brooks, T.M. (2018). Land Use Intensity-specific Global

573   Characterization Factors to Assess Product Biodiversity Footprints. Environ. Sci.

574   Technol. *52*, 5094–5104.

575

576 **Figure legends**

577 **Figure 1.** Combined threats from habitat loss and fragmentation to mammal species richness

578 per ecoregion. A) Number of species committed to extinction. B) Proportion of species

579 committed to extinction. Grey = no data. Boxplots indicate the minimum, first quartile, median,

580 third quartile, and maximum of (relative) species loss values per realm. AA = Australasia (83

581 ecoregions), AN = Antarctic (2 ecoregions), AT = Afrotropic (108 ecoregions), IM = Indomalay

582 (106 ecoregions), NA = Nearctic (117 ecoregions), NT = Neotropic (172 ecoregions), OC =

583 Oceania (22 ecoregions), PA = Palearctic (197 ecoregions).

584   **Figure 2.** Predicted mammal species losses per ecoregion. Predicted losses due to A) habitat

585   conversion and B) fragmentation (ecoregions ordered by impact in the bar chart) as well as C)

586   the relative contribution of fragmentation effects to species loss (ecoregions ordered by

587   relative share of habitat conversion effects in bar chart). Grey signifies no data or zero

588   predicted extinctions (in panel C). Note the different colour scales in panels A, B, and C.

589   **Figure 3.** Relationship between predicted habitat fragmentation and habitat loss effects and

590   corresponding Spearman's rank correlation coefficient (ρ). The direction of the relationship is

591   assessed by a linear trend line (grey solid line with 95% confidence interval). The line of

592   equality (dashed) indicates that habitat conversion effects are dominant over the effects of

593   habitat fragmentation.

594   **Figure 4.** SHR predicted species loss compared with the IUCN documented number of

595   extinct and endangered species threatened by land use per ecoregion. The axis scales have

596   been square root-transformed. The plot includes the line of equality (dashed) and the linear

597   trend line (grey solid line including 95% confidence interval). The Spearman's rank correlation

598   coefficient (ρ) describes the correlation of the predicted species loss and the number of

599   extinct and endangered species as documented by the IUCN. Species with IUCN Red List

600   category 'VU', 'EN', 'CR', 'EW', and 'EX' were considered threatened or extinct. Note that

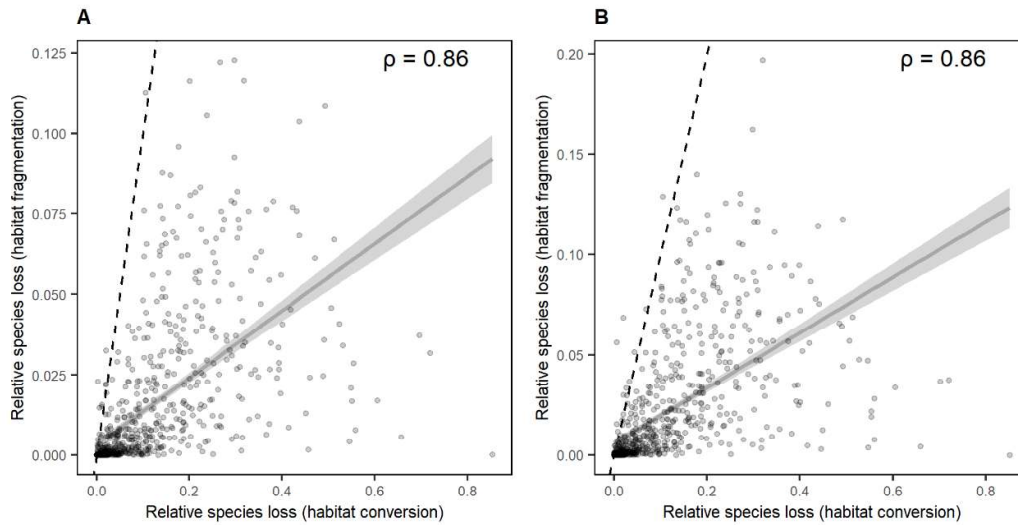601   observations (ecoregions) may overlap, represented by a darker shade of grey.

Supplemental information

603 *Supplemental figures*
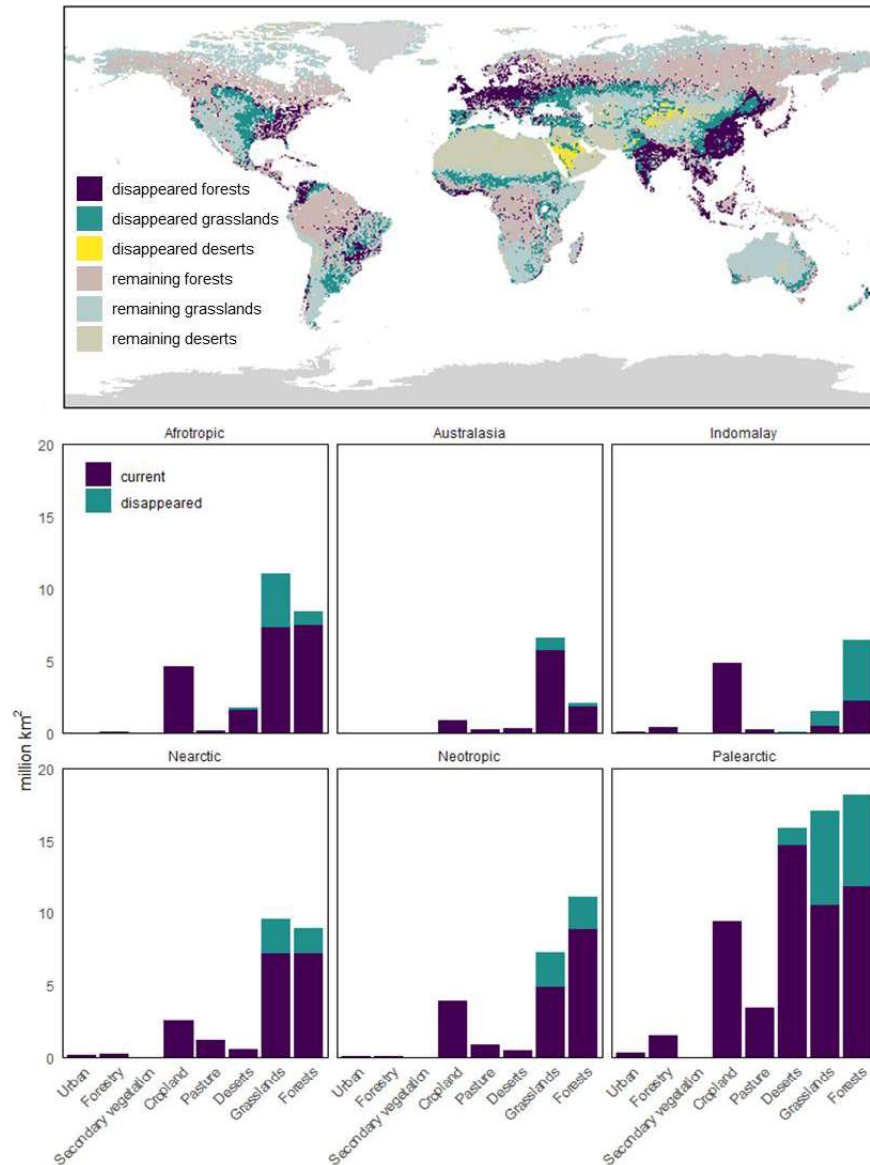
604

605 **Figure S1.** Global land use and land cover change. Global land use and land cover change (grey signifies no data)

606 relative to a natural baseline based on the GLOBIO4 2015 land use map (1) and ISLSCP II Potential Natural

607 Vegetation map (2). The predicted species losses correspond to global declines of 30% and 34% in natural forest and

608 grassland area, respectively, relative to a natural baseline. Further, the effectively connected forest and grassland

609 area has declined by 33% and 37%, respectively, indicating that the remaining forests and grasslands have become

610 increasingly fragmented. This is illustrated by the increase in number of forest fragments from 0.74 million to 0.99

611 million, decrease in mean patch size from 75 km^2 to 39 km^2, and an increase of the mean regional inter-patch

612 distance from 21 km to 29 km. Global grasslands fragments show a similar pattern.

613

Figure S2. Predicted habitat conversion and habitat fragmentation threats per ecoregion for median and maximum
natal dispersal distances. Effects based on A) maximum natal dispersal distances and B) median natal dispersal
distances. The relationship between habitat conversion and fragmentation effects is assessed by the Spearman's
correlation coefficient (ρ) and the direction of the relationship is indicated by a generalised linear model (grey line)
with a 95% confidence interval. The identity line (dashed) indicates that habitat conversion effects are dominant over
the effects of habitat fragmentation.

A

Afrotropic · Australasia · Indomalay

Nearctic · Neotropic · Palearctic

Species loss (n)

B

Afrotropic · Australasia · Indomalay

Nearctic · Neotropic · Palearctic

Species loss (n)

Ecoregion

Figure S3. Predicted species loss caused by habitat fragmentation. Predicted species loss based on A) maximum natal dispersal distances and B) median natal dispersal distances. The ecoregions are grouped by realm and ordered based on the predicted fragmentation impact. Antarctic and Oceanic ecoregions are excluded because of the absence of fragmentation impacts on absolute species loss.

Relative contribution of fragmentation effects (−)

0.00   0.25   0.50   0.75

Fragmentation effects   Habitat conversion effects

625

Figure S4. Relative contribution of fragmentation threats to predicted species loss based on median natal dispersal

distances. Grey signifies no data or zero predicted extinctions.

Figure S5. Predicted species loss per ecoregion according to the SHR, assuming A) minimum species accumulation

rates (lower 90% confidence interval of z-value), B) a mean species accumulation rate, and C) maximum species

accumulation rates (upper 90% confidence interval of z-value) compared with the documented number of extinct and

endangered ('VU', 'EN', 'CR', 'EW', 'EX') species threatened by land use according to IUCN. The axis scales have

been square root-transformed. The line of equality is shown dashed, and the trend line is shown in grey (including

95% confidence intervals). The Spearman's rank correlation coefficient (ρ) describes the correlation of the predicted

species loss and IUCN documentation on extinct and endangered species.

637 *Supplemental **tables***

638 **Table S1**. Regional slopes (*z* values) of the SHR curves. Slopes for the ecoregions within each biome of the species-

639 habitat relationship, derived from Kehoe et al. [34]. The global *z* value reported by Kehoe et al. [34] is 0.22.

Biome	SHR slope (*z*)	Lower 90% CI	Upper 90% CI
Tropical & subtropical moist broadleaf forests	0.17	0.09	0.25
Tropical & subtropical dry broadleaf forests	0.26	0.08	0.44
Tropical & subtropical coniferous forests	0.49	0.00	1.00
Temperate broadleaf & mixed forests	0.20	0.12	0.28
Temperate conifer forests	0.20	0.10	0.30
Boreal forests/taiga	0.14	0.07	0.21
Tropical & subtropical grasslands, savannas & shrublands	0.21	0.13	0.29
Temperate grasslands, savannas & shrublands	0.20	0.07	0.33
Flooded grasslands & savannas	0.23	0.00	0.46
Montane grasslands & shrublands	0.27	0.11	0.43
Tundra	0.21	0.11	0.31
Mediterranean forests, woodlands & scrub	0.26	0.11	0.41
Deserts & xeric shrublands	0.21	0.13	0.29
Mangroves	0.23	0.02	0.44

640

641 **Table S2.** Mean and maximum predicted regional species loss (and relative contribution of fragmentation effects to

642 species loss) in the three different z-value scenarios (lower 90% confidence interval, mean, and upper 90%

643 confidence interval.

Measure	Lower 90% CI	Mean CI	Upper 90% CI
Mean absolute species loss	5	10	13
Maximum absolute species loss	68	86	105
Mean relative species loss	6%	11%	14%
Maximum relative species loss	86%	85%	85%
Mean relative contribution of fragmentation effects	10%	9%	9%
Maximum relative contribution of fragmentation effects	90%	90%	90%

644

645 **Table S3.** Predicted regional species loss (and relative contribution of fragmentation effects to species loss) in
646 selected ecoregions using three land cover resolutions (300 m, 1 km, and 3 km).

Realm	Region (ID)	Area (km²)	Species loss (relative loss)			Contribution of fragmentation effects		
			300 m	1 km	3 km	300 m	1 km	3 km
Afrotropic	Mandara Plateau mosaic (30710)	7479	33 (48%)	35 (51%)	37 (55%)	6%	5%	3%
Indomalay	Sumatran tropical pine forests (40304)	2748	7 (7%)	7 (7%)	7 (7%)	10%	9%	1%
Neotropic	Tehuacán Valley matorral (61316)	9862	17 (17%)	17 (18%)	17 (18%)	16%	14%	12%
Nearctic	Florida sand pine scrub (50513)	3879	5 (12%)	5 (12%)	5 (13%)	1%	1%	1%

647

648

649   **Table S4.** Land type aggregation of the GLOBIO4 [22] land use and ISLSCP PNV [51] land cover maps.

ID	land type	GLOBIO ID	GLOBIO4 land type	PNV ID	PNV land cover type
0	No data	0	No data	16	No data
1	Urban	1	Urban		
2	Cropland	230	Cropland, light use		
		231	Cropland, intense use		
3	Pasture	3	Pasture, intense use		
		4	Pasture, light use*		
4	Forestry	5	Forestry		
11	Forests	50	Tree cover, broadleaved, evergreen, closed to open (>15%)	1	Tropical evergreen forest
		60	Tree cover, broadleaved, deciduous, closed to open (>15%)	2	Tropical deciduous forest
		61	Tree cover, broadleaved, deciduous closed (>40%)	3	Temperate broadleaf evergreen forest
		62	Tree cover, broadleaved, deciduous, open (15-40%)	4	Temperate needleleaf evergreen forest
		70	Tree cover, needle leaved, evergreen, closed to open (>15%)	5	Temperate deciduous forest
		71	Tree cover, needle-leaved, evergreen, closed (>40%)	6	Boreal evergreen forest
		72	Tree cover, needle-leaved, evergreen open (15-40%)	7	Boreal deciduous forest
		80	Tree cover, needle -leaved, deciduous, closed to open (>15%)	8	Mixed forest
		81	Tree cover, needle-leaved, deciduous, closed (>40%)		
		82	Tree cover, needle-leaved, decidu1ous, open (15-40%)		
		90	Tree cover, mixed leaf type (broadleaved and needle-leaved)		
		100	Mosaic tree and shrub (>50%) / herbaceous cover (<50%)		
		160	Tree cover, flooded, fresh or brackish water		
		170	Tree cover, flooded, saline water		
12	Grasslands	110	Montane Grasslands and Shrublands [agg]; Mosaic tree and shrub (>50%) / herbaceous cover (<50%) [crop]	9	Savanna
		120	Shrubland	10	Grassland/steppe
		121	Evergreen shrubland	11	Dense shrubland
		122	Deciduous shrubland	12	Open shrubland
		130	Grassland	13	Tundra
		140	Lichens and mosses		
		150	Sparse vegetation (tree, shrub, herbaceous cover) (<15%)		
		151	Sparse tree cover (<15%)		
		152	Sparse shrub (<15%)		
		153	Sparse herbaceous cover (<15%)		
		180	Shrub or herbaceous cover, flooded, fresh/saline/brackish water		
13	Deserts	200	Bare areas	14	Desert
		202	Unconsolidated bare areas		
15	Water bodies	210	Water bodies	0	Water bodies
16	Rock & ice	201	Consolidated bare areas	15	Polar desert/rock & ice
		220	Permanent snow and ice		

650   * The GLOBIO4 "Pasture, light use" class was replaced by the original ESA European Space Agency Climate

651   Change Initiative landcover [49], resulting in replacement by one of the natural landcover types (GLOBIO4 ID 50-180,

652   199-220).

Supplemental references

653

654   1.   A. M. Schipper, et al., Projecting terrestrial biodiversity intactness with GLOBIO 4.

655   Glob. Chang. Biol. 26, 760–771 (2020).

656   2.   N. Ramankutty, et al., "ISLSCP II Potential Natural Vegetation cover" (2010)

657   https:/doi.org/https://doi.org/10.3334/ORNLDAAC/961.

658   3.   IUCN, The IUCN Red List of Threatened Species. Version 2020-2 (2020) (August 15,

659   2020).

660   4.   ESA, Land Cover CCI Product, User Guide Version 2.0. 1–104 (2017).

661   5.   L. Kehoe et al., Agriculture rivals biomes in predicting global species richness.

662   Ecography 40(9), 1118–1128 (2017).

663

Science for society

Over 77% of the Earth's land cover has been affected by human activity, reducing and fragmenting the amount of suitable habitat for wildlife. We apply a predictive species-area model to land cover maps, non-flying mammal species habitat preferences and dispersal capacities, to assess the loss and change in connectivity of remaining habitat across the world's terrestrial ecoregions (i.e., regions delineated by homogeneity of species pools) and assess its consequences for regional mammal species loss. We predict that due to present-day land use an average of 10 mammal species will extirpate across the ecoregions, although this can be up to 86 in a highly affected, large, and biodiverse ecoregion. Change in habitat connectivity contributes on average 10% to the total predicted threats from land use, but this can be up to 90% in highly fragmented landscapes. The ability to predict large-scale landscape configuration effects on regional species diversity is a pivotal component of an integrated area-based conservation strategy for meeting internationally agreed targets for halting or restoring biodiversity loss.
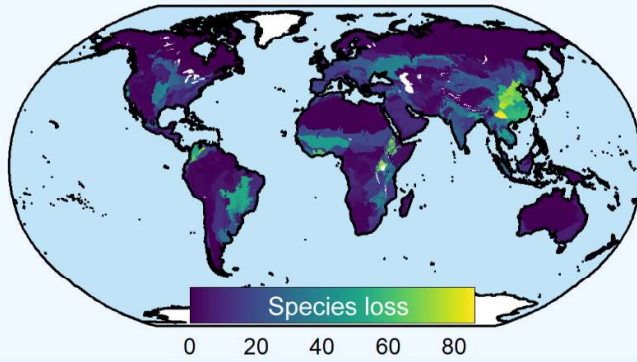
Highlights

- We predict an average of 10 (max = 86) ecoregional mammal extinctions due to human land use
- On average, 10% of the loss is caused by fragmentation, yet this can be up to 90%
- Threats from habitat loss and fragmentation are strongly correlated
- Measures to protect biodiversity should consider both habitat loss and fragmentation

eTOC blurb

We use a species-area model that accounts for habitat quality and patch connectivity to assess the threats from present-day habitat loss and fragmentation to non-volant mammal species richness across the world's ecoregions. We predict an average of 10 species extirpations due to habitat loss (generally constituting 90% of the impacts) and fragmentation (10%). Our results imply that comprehensive strategies for meeting international biodiversity targets require not only combatting habitat loss, but also measures to reduce fragmentation.

691 **Graphical abstract**

- Modelling habitat loss and fragmentation effects on mammal diversity across 804 ecoregions
- Considering distribution, habitat use, and dispersal distance of 4,179 non-volant mammal species
- Average of 10 predicted regional extinctions due to habitat loss and fragmentation
- Habitat fragmentation predicted to cause on average 10% of the species loss (but up to 90%)

Species loss

0   20   40   60   80

692

1   **Habitat fragmentation amplifies threats from habitat loss to**

2   **mammal diversity across the world's terrestrial ecoregions**

3   Koen JJ Kuipers[1,2*], Jelle P Hilbers[2], John Garcia-Ulloa[3], Bente J Graae[4], Roel May[5],

4   Francesca Verones[1], Mark AJ Huijbregts[2], Aafke M Schipper[2,6].

5   [1] Industrial Ecology Programme, Department of Energy and Process Engineering, NTNU, 7034 Trondheim, Norway

6   [2] Department of Environmental Science, Radboud University, 6526 AJ Nijmegen, the Netherlands

7   [3] Institute of Terrestrial Ecosystems, Department of Environmental Systems Science, ETH, 8092 Zürich, Switzerland

8   [4] Department of Biology, NTNU, 7491 Trondheim, Norway

9   [5] Department of Terrestrial Ecology, Norwegian Institute for Nature Research (NINA), 7485 Trondheim, Norway

10   [6] PBL Netherlands Environmental Assessment Agency, 2594 AV the Hague, the Netherlands

11   [*] Lead contact and correspondence: koen.kuipers@ru.nl

12   **Summary**

13   Global biodiversity is increasingly threatened by anthropogenic environmental change. At

14   present, 25% of comprehensively assessed species are threatened with extinction. While

15   there is mounting evidence that habitat loss is a key threat to biodiversity, global assessments

16   typically ignore additional threats from habitat fragmentation. Here, we present a new

17   species-area model that integrates habitat size and habitat connectivity, accounting for

18   species habitat preference, patch size, inter-patch distances, landscape matrix permeability

19   and species' dispersal capacity. We applied the model to predict the combined threat from

20   habitat loss and fragmentation to non-volant mammal species richness in 804 of the world's

21   terrestrial ecoregions. We predict that on average across the ecoregions, 10 mammal species

22   are committed to extinction due to habitat loss and fragmentation combined (range 0-86). On

23   average, 9% of the predicted species loss is due to fragmentation (range 0-90%). Considering

24   bot habitat loss and fragmentation, our model can be used for large-scale explorative

25   assessments to inform and evaluate strategies for minimising biodiversity loss due to the

26   expansion of human land use and for optimizing habitat conservation and restoration.

27   **Keywords**

28   Biodiversity, habitat connectivity, habitat conversion and fragmentation, land use, Mammalia,

29   species extinctions, species-area relationship.

Introduction

Due to the increasing human pressure on the natural environment, current species extinction rates are significantly higher than background rates, suggesting that we have entered a sixth mass extinction event [1,4]. At present 25% of the species comprehensively assessed by the International Union for the Conservation of Nature (IUCN) are threatened with extinction [1].

Habitat conversion has been identified as the predominant threat to biodiversity [1,6]. Time series of satellite observations reveal a rapid expansion of human land use at the cost of natural land cover [8,10,11]. Currently, over 77% of the terrestrial land cover has been affected by human activity [10], severely reducing the intactness of natural habitat [12,13], and scenario projections point at imminent further habitat conversion [14].

Global effects of habitat loss on biodiversity have been assessed in various recent studies, for example by synthesising local field observations [15], applying habitat suitability models [16,17], or by using species-area relationships (SARs) [18]. These assessments, however, generally ignore potential additional effects of habitat fragmentation, which may exacerbate biodiversity loss because populations in smaller and more isolated fragments are typically less viable [19,20]. As measures to combat habitat loss and fragmentation may differ [21], methods to estimate relative and combined effects of habitat loss and fragmentation globally are imperative to inform strategies to halt or reverse global biodiversity loss. This, in turn, is particularly relevant against the background of the upcoming post-2020 Global Biodiversity Framework [22].

Assessing effects of habitat loss and fragmentation on species diversity is complex, mainly due to variability in species' responses [23]. Fragmentation effects on species diversity are commonly studied via regression analyses relating empirical data on species diversity to habitat fragmentation variables (e.g., [19,24–26]). These empirical relationships can be combined with global land use maps to estimate global effects of fragmentation on local species diversity (e.g., [5]). Global estimates of assemblage-level responses to habitat loss and fragmentation can complement local, species-specific assessments to underpin large-scale strategies to combat negative biodiversity trends [1].

SAR models are commonly used to obtain global estimates of the threats from habitat loss to regional species diversity, generating estimates of imminent and longer-term future

59   extinctions of species that cannot persist given the size of the remaining habitat [1,18]. Although

60   SAR models are continuously being refined [27,28], they generally ignore connectivity between

61   habitat fragments [18,29]. Recently, Garcia-Ulloa et al. [30] proposed to combine species-area

62   models with the equivalent connected area (ECA) concept [31]. The ECA is a measure of area

63   weighted by its connectivity based on habitat fragment sizes and the probability of species'

64   dispersal between the fragments. The probability of dispersal is derived from the distance

65   between the fragments, permeability of the intermediate landscape matrix, and species'

66   dispersal capacity [32]. The ECA equals the total habitat area if all fragments are fully

67   connected, while it approaches the size of the largest single fragment if the fragments

68   become increasingly isolated.

69   Here, we present and apply a new SAR model that incorporates the ECA into the countryside

70   SAR (c-SAR) [27]. This integrated model, from hereon called the species-habitat relationship

71   (SHR), allows to systematically evaluate and compare threats from habitat loss and

72   fragmentation as it accounts for both habitat suitability (via the c-SAR model) and habitat

73   connectivity (via the ECA concept). By incorporating the ECA concept, the SHR considers

74   various relevant aspects of habitat fragmentation, including patch size, connectivity, and

75   matrix quality. Other fragmentation aspects, such as edge effects, are however not captured.

76   We applied the SHR model to evaluate threats from habitat loss and fragmentation on non-

77   volant mammal species diversity across the world's ecoregions ecoregions. We find that

78   threats from habitat loss are generally dominant over fragmentation threats, but that

79   fragmentation has a significant contribution and may even dominate the combined threat in

80   ecoregions characterised by severely fragmented habitats. Hence, considering habitat

81   fragmentation is relevant in global biodiversity assessments and for optimising area-based

82   conservation strategies.

83   **Results**

84   ***Threats from habitat loss and fragmentation combined***

85   The current global loss and fragmentation of natural habitat (as based on a land-use map for

86   2015; Fig. S1) corresponds with an average predicted loss of 10 mammal species across the

87   ecoregions (range = 0-86 species), equal to a relative loss of 11% on average (range = 0-

88   85%) (Fig. 1). In 578 of the 804 ecoregions (72%), at least one mammal species was

89   predicted to become regionally extinct. Predicted species loss was highest in the Yunnan

90   Plateau subtropical evergreen forests (species loss = 86), Sichuan Basin evergreen broadleaf

91   forests (species loss = 78), and Magdalena Valley dry forests (species loss = 77) ecoregions.

92   Relative species loss was predicted to be highest in Patía Valley dry forests (relative loss =

93   0.85), Magdalena Valley dry forests (relative loss = 0.75), and Cauca Valley dry forests

94   (relative loss = 0.73) ecoregions (see Data S2 for a complete overview of ecoregion-specific

95   results). Palearctic, Afrotropic, and Indomalayan ecoregions were predicted to be the most

96   affected and Oceanic and Australasian ecoregions the least, in terms of both absolute and

97   relative numbers of predicted extinctions. The similarity in the global patterns of absolute and

98   relative predicted species losses (Fig. S2) indicates that absolute species loss is determined

99   by the extent of land conversion and fragmentation rather than inherent differences in species

100   richness among the ecoregions.

101   ***Contribution of habitat fragmentation***

102   The threats from habitat loss were generally dominant over the threats from fragmentation

103   (Fig. 2). On average across the ecoregions, habitat loss corresponded with a predicted loss of

104   nine species (range = 0-78), while fragmentation accounted for one additional extinction

105   (range = 0-18) and 9% of the combined threat. In 75 ecoregions (9%), fragmentation was

106   predicted to account for ≥25% of the combined threat and in 11 ecoregions (1%),

107   fragmentation threats contributed ≥50% (e.g., in the Guianan Piedmont and lowland moist

108   forests, Australian Alps montane grasslands, and Sulawesi lowland rain forests ecoregions;

109   Data S2). In 321 ecoregions (40%), fragmentation was predicted to cause at least one

110   additional mammal extinction. We further found a positive correlation between habitat loss

111   and fragmentation threats (Fig. 3), reflecting that more habitat conversion generally brings

112   about more fragmentation.

113   ***Comparison with IUCN Red List***

114   Our average estimate of 10 predicted ecoregion-level extinctions (11%) is similar to the

115   estimate of the IUCN Red List [2], which reports on average eight species as extinct or

116   endangered and threatened by land use, corresponding to an average of 10% of the

117   ecoregional species pool. Further, we found a Spearman's rank correlation coefficient (ρ) of

118   0.49 between the numbers of extinct and endangered species predicted by our model and

119   estimated by the IUCN (Fig. 4).

120   Our assessment of fragmentation impacts provides a conservative estimate as we based our

121   calculations on species' maximum natal dispersal distance. Using the median natal dispersal

122   distance instead, we found on average two predicted extinctions (range = 0-19) due to

123   fragmentation instead of one (for details see the supplemental methods and Fig. S3). The

124   total number of predicted extinctions was similar (10 species in both dispersal scenarios, and

125   ranges of 0-86 and 0-88 in the maximum and median natal dispersal distance scenarios,

126   respectively), but the average contribution of fragmentation effects increased from 9% to 13%

127   (Fig. S4). Using the median rather than the maximum natal dispersal distance did not affect

128   the correlation between predicted and observed numbers of extinct and endangered species

129   (Spearman's ρ = 0.49; Fig. S5) or the relationship between predicted habitat conversion and

130   fragmentation effects (Fig. S2).

131   ***Sensitivity analysis***

132   To assess the sensitivity of our model results to uncertainty in the slope of the SHR, we

133   performed additional calculations based on the 90% confidence intervals (CI) of the slope

134   values of the SHR, i.e. the species-area accumulation rates (Table S1). Changes in slope

135   values did not affect the predicted contribution of fragmentation effects, which remained on

136   average 9-10% (range = 0-90%; Table S2). The correlation between predicted and

137   documented numbers of extinct and endangered species also hardly changed by using

138   different slopes values (ρ = 0.43-0.51; Fig. S5). Global average predicted species loss,

139   however, changed by ±4 species (corresponding to ±4%) when adopting lower or upper 90%

140   CI slope values (with higher slope values resulting in higher predicted species loss; Table

141   S2).

142   As we applied the SHR to a global land-use map aggregated to a 1 km resolution (30"), our

143   assessment omits habitat patches smaller than 0.5 km^2 that could act as stepping stones and

144   thus improve habitat connectivity. To test the sensitivity of our results to the spatial resolution

145   of the land-use map, we applied the SHR at 300 m, 1 km, and 3 km resolutions for four small

146   ecoregions across different realms that are disproportionally affected by fragmentation. We

147 found that the average contribution of fragmentation effects increased from 4% at a low

148 resolution (3 km) to 8% at a high resolution (300 m; Table S3).

149 **Discussion**

150 Habitat loss is considered the main threat to biodiversity globally. Nevertheless, effects of

151 fragmentation are typically ignored in global biodiversity assessments, leading to a potential

152 underestimation of extinction risks. Here, we proposed and applied a method to estimate the

153 relative and combined threats from habitat loss and fragmentation to the diversity of non-

154 volant mammal species across the world's terrestrial ecoregions. Our results suggest that the

155 threats from habitat loss are generally dominant. This finding was independent of the

156 assumptions made with regard to species' dispersal capacity and slopes of the SHR (e.g.,

157 Figs S3-S5). Yet, we predicted that fragmentation threats are not negligible. Hence, land use

158 impact assessments that ignore additional fragmentation effects may systematically

159 underestimate species loss. Our ecoregion-level predictions indicate that the threats are

160 underestimated by about 10% on average, but the underestimation can be up to 90% in

161 highly fragmented ecoregions. In the Madagascar subhumid forests and the Sulawesi lowland

162 rain forests, for example, the predicted threats from fragmentation constitute more than half of

163 the total threats from habitat change, reflecting a highly fragmented remaining forest cover.

164 Divergent species responses to fragmentation may have contributed to the ongoing debate on

165 the relative significance of threats from habitat conversion and fragmentation [33–35]. We

166 estimated assemblage-level threats from habitat conversion and fragmentation across the

167 globe using a species-area model that consistently accounts for both the suitability and

168 connectivity of habitat. Turning off the threats of habitat fragmentation in our SHR model

169 enabled us to estimate the relative threats from habitat loss and fragmentation. Although we

170 found threats from habitat loss to be dominant over threats from habitat fragmentation,

171 predicted extinctions were higher in ecoregions with more fragmented habitat. This supports

172 conclusions from Haddad et al. [19] and Crooks et al. [20]. Furthermore, our results are in line with

173 local evidence from estimates of the impacts of forest fragmentation in Borneo, where

174 reduced functional connectivity for forest vertebrates imposed an additional 7% loss of

175 functional habitat [36].

176   For individual ecoregions, the total species loss predicted by the SHR may deviate from the

177   number of extinct and endangered species documented by the IUCN (Fig. 4). The IUCN data

178   are based on extinction risk assessments at the species level, whereas the SHR models net

179   changes in regional species richness (which may not reflect species-specific changes in a

180   specific location). Where possible, we parameterised the SHR based on the species pool

181   specific to each ecoregion (i.e., for land type suitability, matrix permeability, and body mass-

182   specific dispersal distance). Furthermore, we specified the species-area accumulation rates

183   (z) using mammal-specific values differentiated according to biome (Table S1; [3]). Yet, our

184   model does not cover all aspects that may influence projected species losses, including

185   species-specific dispersal behaviour, species' distributions within ecoregions, or differences in

186   species' accumulation rates among vegetation types. Additionally, we based our model

187   estimates on a relatively crude binary habitat classification scheme where a land type is either

188   suitable or unsuitable for a given species [2], whereas in reality species exhibit more subtle

189   differences in habitat use that need not align with simple land cover classes. Further, IUCN

190   threat levels are global in scope, which may cause a mismatch with the ecoregion-specific

191   SHR predictions (i.e., species could be more threatened in one ecoregion than in another).

192   Finally, the SHR considers effects of change in patch size, connectivity, and matrix quality,

193   and does therefore not incorporate other relevant aspects of fragmentation, such as edge

194   effects. Moreover, the SHR considers effects of habitat conversion only, and neglects threats

195   to species other than those caused by land use, such as overexploitation, pollution, or climate

196   change. Species covered by the IUCN can be endangered due to a variety of human

197   stressors in addition to habitat conversion [2]. Despite the deviations at ecoregion level,

198   however, we found a Spearman's rank correlation coefficient (ρ) between the SHR

199   predictions and IUCN data of 0.49 (Fig. 4) and a good match on average (10 vs 8 species

200   extinct or endangered). This suggests that our model can be used for large-scale exploratory

201   assessments of the threats from habitat loss and fragmentation on mammal species richness,

202   for example in comparative scenario projections [37,38], but it also highlights that predictions at

203   the ecoregional level are associated with uncertainty.

204   Yet, the non-negligible contribution of fragmentation to the predicted species loss emphasises

205   the need for more comprehensive assessments of land cover change effects on biodiversity.

206   Complementing mechanistic approaches assessing population-level responses [39], the SHR

207   provides an opportunity to systematically assess combined threats from habitat loss and

208   fragmentation on species richness across large extents, as it is relatively easily parametrised

209   for different species groups and spatial units by adapting the SHR species-accumulation

210   rates, land type suitabilities and dispersal capacities. Using the SHR in combination with land

211   use scenarios would allow for estimating the consequences of different land use 'futures',

212   including further conversion of natural habitat as well as restoration. This can inform and help

213   to evaluate strategies for minimising effects of expansion of human land use, support habitat

214   restoration programs, or contribute to the effective allocation and design of conservation and

215   protected areas in combination with prioritisation procedures [40]. Our comparative assessment

216   across three spatial resolutions indicates that predictions with the SHR model are preferably

217   made based on high-resolution land use maps. Coarse resolutions may aggregate small

218   fragmented patches to a larger single patch (similar to functionally connected patches).

219   Hence, application at coarse resolutions may underestimate fragmentation. This indicates the

220   importance of small habitat patches as stepping stones in the landscape [41].

221   Curtailing biodiversity loss rates requires acute and significant conservation efforts. As most

222   targets set within the Strategic Plan for Biodiversity 2011-2020 have not been reached, there

223   are major challenges in the ongoing negotiations towards a post-2020 Global Biodiversity

224   Framework [22]. Given that land use is a key driver of biodiversity loss and that feeding the

225   growing human population may further increase the demand for land, there is a key role for

226   strategies to minimise impacts of habitat conversion on biodiversity and ecosystems [42,43].

227   Combining the SHR with global land use projections would enable evaluating the effects of

228   both the amount and spatial configuration of habitat. In turn, this information can play a role in

229   designing comprehensive conservation strategies based on contrasting paradigms and

230   corresponding measures (e.g., sparing versus sharing; [44,45]). The ability to predict large-scale

231   landscape configuration effects on regional species diversity is a pivotal component towards

232   designing area-based conservation strategies for meeting internationally agreed targets for

233   halting or restoring biodiversity loss. These large-scale assessments should in turn be

234   complemented by an understanding of local and species-specific responses to habitat loss

235   and fragmentation, which do not necessarily correspond with the large-scale assemblage-

236   level patterns (e.g., [19,25,26,46,47]). Improved understanding of biodiversity change at global,

237   regional, and local scales is key for identifying comprehensive and targeted conservation

238   measures and meeting biodiversity targets [48].

239   **Experimental procedures**

240   ***Resource availability***

241   *Lead contact*

242   Further information and requests for resources should be directed to and will be fulfilled by

243   the lead contact, Koen Kuipers (koen.kuipers@ru.nl).

244   *Materials availability*

245   The datasets with habitat affinity, matrix conductivity, and dispersal distance (Data S1), and

246   ecoregional habitat data (i.e., equivalent connected area, species richness, habitat suitability,

247   species-accumulation rates, and dispersal distances; Data S2) have been deposited to

248   Figshare under doi.org/10.6084/m9.figshare.16616650.v1.

249   *Data and code availability*

250   All original data used in this research are publicly available. Species distribution spatial data

251   and habitat documentation data are deposited by IUCN Red List of Threatened Species.

252   Mammal species body mass data are deposited on Figshare under

253   doi.org/10.6084/m9.figshare.c.3306933.v1. Ecoregion spatial data area deposited by WWF

254   under doi.org/10.1641/0006-3568(2001)051[0933:TEOTWA]2.0.CO;2. 2015 land-use and

255   land cover spatial data is deposited by the GLOBIO project under doi.org/10.1111/gcb.14848.

256   The European Space Agency (ESA) Climate Change Initiative (CCI) land cover (LC) data is

257   deposited by the ECA-CCI-LC and publicly available upon request at http://www.esa-

258   landcover-cci.org/?q=node/164. The potential natural vegetation data is deposited by the Oak

259   Ridge National Laboratory (ORNL) Distributed Active Archive Center (DAAC) under

260   doi:10.3334/ORNLDAAC/961.

261   Code treating the raw data to parametrise the SHR and generate results of this publication

262   (Code S1-3) are available in on Figshare under doi.org/10.6084/m9.figshare.16616650.v1.

263 ***Model description***

264 The species-habitat relationship (SHR) models the relationship between the number of

265 species committed to extinction and the suitability and spatial configuration of various land-

266 use and land cover types (hereafter referred to as land types). It is an integration of the

267 countryside SAR (c-SAR) [27] and the equivalent connected area (ECA) concept [31] such that

268 the area variable of the conventional c-SAR is replaced by the ECA [30]. The differential

269 suitability of various land types considered in the c-SAR can be considered equivalent to

270 matrix permeability, which in turn is a key parameter in the ECA. Thus, the integration of c-

271 SAR and ECA allows for consistent modelling of land type suitability and matrix permeability

272 across all ecoregions, considering that distinct land types host different species groups and

273 that some species may occur across several land types.

274 Similar to how the c-SAR can be used to estimate relative species loss (RSL) due to habitat

275 loss [18,29], the SHR can be used to estimate RSL due to both habitat conversion and

276 fragmentation (equation 1), as

277 (1) $\quad RSL = 1 - \left(\frac{\sum_i h_i \cdot ECA_i}{\sum_i h_i \cdot ECA_{i,ref}} \right)^z$

278 where h_i is the suitability of land type i, ECA_i is the ECA of land type i, $ECA_{i,ref}$ is the ECA of

279 land type i in the reference landscape (i.e., no human land use), and z is the slope (i.e.,

280 species accumulation rate) of the species-habitat curve. Absolute species loss can be

281 quantified by multiplying the RSL with the number of species in the reference state.

282 Land type suitabilities (h) are defined as the proportion of species occurring in land type i

283 relative to the total number of species in the region, raised to the power 1/z (equation 2) [18].

284 (2) $\quad h_i = \left(\frac{s_i}{s} \right)^{1/z}$

285 The *ECA* considers the spatial configuration of the landscape and the degree of

286 fragmentation as perceived by the species group occurring in land type i. The *ECA* is based

287 on the number and size (a) of individual habitat patches m and n of land type i and the

288 probability of dispersal (p) between each pair of patches m and n (equation 3).

289 (3) $\quad ECA_i = \left(\sum_{m,n} a_{i,m} \cdot a_{i,n} \cdot p_{i,mn} \right)^{0.5}$

290 The probability of dispersal (p) among patches of land type i is defined by the dispersal kernel

291 based on the least-cost distance (w) between habitat patches m and n and the dispersal

292 distance (α) of the species occurring in land type i [49] (equation 4).

293 (4) $\quad p_{i,mn} = e^{-w_{i,mn}/\alpha_i}$

294 The least-cost distance (w) is defined as the permeability-weighted length of the route that

295 results in the shortest distance between patch m and n [32] by multiplying the distance d

296 travelled through landscape matrix type k by the resistance (r) of the matrix type (equation 5)

297 [30]. Relatively permeable matrix types form so-called "stepping stones", improving the

298 connectivity of distant patches [32].

299 (5) $\quad w_{i,mn} = \sum_k d_{i,mn,k} \cdot r_{i,k}$

300 The permeability of the matrix separating the habitat patches of land type i is based on the

301 overlap of species between land type i and matrix type k (i.e., the number of species

302 occurring in both land type i and matrix type k; equation 6).

303 (6) $\quad r_{i,k} = 1 - \dfrac{s_{i,k}}{s_i}$

304 If species that occur in land type i all occur in matrix type k, the permeability equals 1 (i.e., a

305 resistance of 0), meaning that this matrix type can be crossed without any cost. Hence, the

306 connectivity of the landscape depends on the species overlap between the land types:

307 habitats in regions with large overlap of species communities between land types are more

308 connected than habitats with distinct communities.

309 ***Model parametrisation***

310 We model the threats from land cover change to species richness at the level of ecoregions,

311 i.e., distinct biogeographical units that can be considered relatively homogeneous in their

312 vegetation and species pool [50]. We cover 804 of the 825 terrestrial ecoregions based on

313 available land type and species data. We retrieved the spatial configuration of the land types

314 in each ecoregion, needed to quantify patch area sizes (a) and the spatial configuration of the

315 landscape, from a high-resolution land-use map for 2015 [5]. To reduce computation time, we

316 resampled the land-use map from 10" (300 m near the equator) to 30" (900 m near the

11

317   equator) based on the mode (i.e., majority rule) and aggregated the original land type classes

318   into eight major land types (Table S4). Four land types are anthropogenic (urban, cropland,

319   pasture, and forestry) and four are natural (forests, grasslands, deserts, and rock and ice).

320   We replaced the original class "light use pasture" by the land cover in the underlying

321   European Space Agency Climate Change Initiative land cover [9], as this class indicates

322   natural habitat that is used mainly for extensive grazing [51]. To establish a baseline natural

323   land cover map, we replaced all anthropogenic land cover by natural land cover as defined by

324   the ISLCSP II Potential Natural Vegetation Cover map [7,52]. We retrieved biome-specific

325   mammal species-area accumulation rates from Kehoe et al. [3], ranging from 0.14 (boreal

326   forest ecoregions, n = 28) to 0.49 (tropical and subtropical coniferous forest ecoregions, n =

327   16) (Table S1).

328   We derived land type suitability (h) and matrix resistance values (r) per ecoregion from

329   species' occurrence ranges and species habitat affinities as documented by IUCN of 4,179

330   non-volant mammal species, representing ~90% of all known extant non-volant mammals [2,53].

331   We have excluded flying mammals (bats) because of uncertain and divergent dispersal

332   behaviour in response to fragmentation compared to non-volant mammals [26]. For deriving

333   land type suitability (h) and matrix resistance (r) values, we first obtained the number of non-

334   volant mammal species (S) per ecoregion based on the overlap of IUCN species range maps

335   (n = 4,179) with the ecoregions [2]. We then defined the land type suitability of each land type i

336   in each ecoregion based on the number of species with affinity to that land use type relative to

337   the total number of species in the ecoregion [2]. The subset of species of land type i that also

338   occur in matrix type k was obtained correspondingly.

339   We define dispersal capacities (α) as the median of the maximum natal dispersal distance of

340   the species specific to each ecoregion and land type i. Using the maximum natal dispersal

341   distance is in line with metapopulation theory [54], as it gives an indication of the possibility of

342   species to reach isolated habitat fragments [54]. We retrieved species-specific maximum

343   dispersal distances using allometric relationships between mammal body mass (b) and home

344   range, and home range and maximum natal dispersal capacity, differentiated according to

345   trophic guild [55,56]. For carnivorous mammals, the species-specific maximum dispersal

346   distance is estimated by $\alpha = 40\sqrt{380b^{1.13}}$; for non-carnivorous mammals, the species-specific

347   maximum dispersal distance is estimated by $\alpha = 40\sqrt{54b}$ (where dispersal distance and body

348   mass are in meters and grams, respectively). We extracted species-specific body mass (b)

349   and trophic guild data from the EltonTraits 1.0 database [57].

350   The slope of the SHR (z) indicates the rate at which species richness increases with

351   equivalent connected area. Such species-area slopes are commonly assumed to range

352   between 0.2 and 0.3, depending on geographical location and environmental conditions

353   [18,27,29]. We retrieved mammal- and biome-specific z values from Kehoe et al. [3], who assessed

354   terrestrial mammal species richness in plots of increasing size based on species' range maps.

355   We assessed threats from habitat loss only by ignoring changes in connectivity after habitat

356   conversion (i.e., assuming human-modified land cover to be equally permeably as the original

357   land cover). We assessed the additional threats from fragmentation as the difference between

358   the predicted species loss caused by habitat conversion and fragmentation combined and the

359   predicted species loss caused by habitat conversion only.

360   We validated the predicted threats from habitat conversion and fragmentation per ecoregion

361   against the number of extinct and endangered species as documented by the IUCN [2], similar

362   to previous studies that validated SAR-based models of species loss (e.g., [37,58,59]). We

363   identified the number of non-flying mammal species per ecoregion, listed as "extinct", "extinct

364   in wild", "critically endangered", "endangered", or "vulnerable" and threatened by at least one

365   land-use category (from the categories "commercial development", "agriculture", "pasture",

366   and "plantations") (n = 795) and calculated the proportion relative to the total number of non-

367   volant mammals (n = 3,659) in the region (excluding "data deficient" species). Furthermore,

368   we excluded species listed as threatened due to criteria A1-4de only (n = 17) because these

369   species are threatened due to overexploitation or exotic alien species and would be listed as

370   threatened even if their habitat remains fully intact. We included both extinct and endangered

371   species, because SAR models estimate both materialised and projected extinctions [18]. We

372   then compared our estimates of relative and absolute species extirpations due to the

373   combined effects of habitat conversion and fragmentation with the relative and absolute

374   number of endangered species threatened with land use according to the IUCN.

375 ***Model simulations for sensitivity assessment***

376 We tested the sensitivity of the outcomes to key parameters by considering different

377 assumptions regarding dispersal capacities (α), species-area accumulation rates (*z*), and land

378 use map resolutions.

379 To assess the sensitivity of our outcomes to the dispersal distance parameter (α), we also

380 performed the calculations based on median rather than maximum natal dispersal distances,

381 resulting in lower species mobility and landscape connectivity. We obtained species-specific

382 median natal dispersal distances from corresponding relationships between body mass and

383 dispersal distance (via body mass-home range, and home range-dispersal distance

384 relationships), estimated as $\alpha = 7\sqrt{380b^{1.13}}$ for carnivorous mammals and $\alpha = 7\sqrt{54b}$ for non-

385 carnivorous mammals (where dispersal distance and body mass are in meters and grams,

386 respectively) [55].

387 We assessed the sensitivity of our results to changes in the slope (*z*) of the SHR by applying

388 lower and higher biome-specific *z*-values based on their 90% confidence intervals (capped

389 between 0 and 1; Table S1).

390 Finally, we assessed the effect of the resolution of the land use map. To that end, we applied

391 the SHR to habitat change in four selected small ecoregions across different realms that are

392 disproportionally affected by fragmentation (Table S3), using resolutions of 300 m (10"), 1 km

393 (30"), and 3 km (100").

Author contributions

399 Conceptualisation, K.J.J.K., J.P.H., J.C.U., B.J.G., R.M., F.V., M.A.J.H., and A.M.S.;

400 Methodology (approach, model, and parameter development), K.J.J.K., J.P.H., M.A.J.H., and

401 A.M.S.; Software (code preparation and application), K.J.J.K.; Formal analysis, K.J.J.K.;

402 Writing – original draft, K.J.J.K., M.A.J.H., and A.M.S.; Writing – review & editing, K.J.J.K.,

403 J.P.H., J.C.U., B.J.G., R.M., F.V., M.A.J.H., and A.S.

406   **References**

407   1.   IPBES (2019). Global assessment report of the Intergovernmental Science-Policy

408   Platform on Biodiversity and Ecosystem Services. E. S. Brondízio, J. Settele, S. Díaz,

409   and H. T. Ngo, eds. (IPBES secretariat, Bonn, Germnay; 1144 pages, ISBN: 978-3-

410   947851-20-1): https://ipbes.net/global-assessment.

411   2.   IUCN (2020). The IUCN Red List of Threatened Species. Version 2020-2.

412   http://www.iucnredlist.org.

413   3.   Kehoe, L., Senf, C., Meyer, C., Gerstner, K., Kreft, H., and Kuemmerle, T. (2017).

414   Agriculture rivals biomes in predicting global species richness. Ecography (Cop.). *40*,

415   1118–1128.

416   4.   Ceballos, G., Ehrlich, P.R., and Dirzo, R. (2017). Biological annihilation via the

417   ongoing sixth mass extinction signaled by vertebrate population losses and declines.

418   Proc. Natl. Acad. Sci., 6089–6096.

419   5.   Schipper, A.M., Hilbers, J.P., Meijer, J., Antão, J., Benítez-López, A., de Jonge, M.,

420   Leemans, L., Scheper, E., Alkemade, R., Doelman, J., et al. (2020). Projecting

421   terrestrial biodiversity intactness with GLOBIO 4. Glob. Chang. Biol. *26*, 760–771.

422   6.   Maxwell, S.L., Fuller, R.A., Brooks, T.M., and Watson, J.E.M. (2016). Biodiversity: The

423   ravages of guns, nets and bulldozers. Nature *536*, 143–145.

424   7.   Ramankutty, N., Foley, J.A., Hall, F., Gollatz, G., Meeson, B., Los, S., Brown de

425   Colstoun, E., and Landis, D. (2010). ISLSCP II Potential Natural Vegetation cover.

426   8.   Potapov, P., Hansen, M.C., Laestadius, L., Turubanova, S., Yaroshenko, A., Thies, C.,

427   Smith, W., Zhuravleva, I., Komarova, A., Minnemeyer, S., et al. (2017). The last

428   frontiers of wilderness: Tracking loss of intact forest landscapes from 2000 to 2013.

429   Sci. Adv. *3*, 1–14.

430   9.   ESA (2017). Land Cover CCI Product, User Guide Version 2.0. 1–104.

431   http://maps.elie.ucl.ac.be/CCI/viewer/download/ESACCI-LC-Ph2-PUGv2_2.0.pdf.

432   10.   Watson, J.E.M., Venter, O., Jasmine, L., Jones, K.R., Robinson, J.G., Possingham,

433   H.P., and Allan, J.R. (2018). Protect the last of the wild. Nature *563*, 27–30.

434   11.   Ellis, E.C. (2019). To Conserve Nature in the Anthropocene, Half Earth Is Not Nearly

435   Enough. One Earth *1*, 163–167.

436   12.   Beyer, H.L., Venter, O., Grantham, H.S., and Watson, J.E.M. (2020). Substantial

437   losses in ecoregion intactness highlight urgency of globally coordinated action.

438   Conserv. Lett. *13*, e12692.

439   13.   Williams, B.A., Venter, O., Allan, J.R., Atkinson, S.C., Rehbein, J.A., Ward, M., Di

440   Marco, M., Grantham, H.S., Ervin, J., Goetz, S.J., et al. (2020). Change in Terrestrial

441   Human Footprint Drives Continued Loss of Intact Ecosystems. One Earth *3*, 371–382.

442   14.   Powers, R.P., and Jetz, W. (2019). Global habitat loss and extinction risk of terrestrial

443   vertebrates under future land-use-change scenarios. Nat. Clim. Chang. *9*, 323–329.

444   15.   Newbold, T., Hudson, L.N., Hill, S.L., Contu, S., Lysenko, I., Senior, R. a, Börger, L.,

445   Bennett, D.J., Choimes, A., Collen, B., et al. (2015). Global effects of land use on local

446   terrestrial biodiversity. Nature *520*, 45–50.

447   16.   Visconti, P., Bakkenes, M., Baisero, D., Brooks, T., Butchart, S.H.M., Joppa, L.,

448   Alkemade, R., Di Marco, M., Santini, L., Hoffmann, M., et al. (2014). Projecting Global

449   Biodiversity Indicators under Future Development Scenarios. Conserv. Lett. *9*, 5–13.

450   17.   Baisero, D., Visconti, P., Pacifici, M., and Cimatti, M. (2020). Projected Global Loss of

451   Mammal Habitat Due to Land-Use and Climate Change Projected Global Loss of

452   Mammal Habitat Due to Land-Use and Climate Change. One Earth *2*, 578–585.

453   18.   Martins, I.S., and Pereira, H.M. (2017). Improving extinction projections across scales

454   and habitats using the countryside species-area relationship. Nat. Sci. Reports *7*, 1–7.

455   19.   Haddad, N.M., Brudvig, L. a., Clobert, J., Davies, K.F., Gonzalez, A., Holt, R.D.,

456   Lovejoy, T.E., Sexton, J.O., Austin, M.P., Collins, C.D., et al. (2015). Habitat

457   fragmentation and its lasting impact on Earth's ecosystems. Sci. Adv. *1*, 1–9.

458   20.   Crooks, K.R., Burdett, C.L., Theobald, D.M., King, S.R.B., Di Marco, M., Rondinini, C.,

459   and Boitani, L. (2017). Quantification of habitat fragmentation reveals extinction risk in

460   terrestrial mammals. Proc. Natl. Acad. Sci. *114*, 7635–7640.

461   21.   Wei, F., Swaisgood, R., Hu, Y., Nie, Y., Yan, L., Zhang, Z., Qi, D., and Zhu, L. (2015).

462   Progress in the ecology and conservation of giant pandas. Conserv. Biol. *29*, 1497–

463   1507.

464 22. Nature Editorial (2020). New biodiversity targets cannot afford to fail. Nature *578*, 337–

465 338.

466 23. Ewers, R.M., and Didham, R.K. (2005). Confounding factors in the detection of

467 species responses to habitat fragmentation. Biol. Rev. *81*, 117–142.

468 24. Martensen, A.C., Ribeiro, M.C., Banks-Leite, C., Prado, P.I., and Metzger, J.P. (2012).

469 Associations of Forest Cover, Fragment Area, and Connectivity with Neotropical

470 Understory Bird Species Richness and Abundance. Conserv. Biol. *26*, 1100–1111.

471 25. Keinath, D.A., Doak, D.F., Hodges, K.E., Prugh, L.R., Fagan, W., Sekercioglu, C.H.,

472 Buchart, S.H.M., and Kauffman, M. (2017). A global analysis of traits predicting

473 species sensitivity to habitat fragmentation. Glob. Ecol. Biogeogr. *26*, 115–127.

474 26. Lino, A., Fonseca, C., Rojas, D., Fischer, E., and Ramos Pereira, M.J. (2019). A meta-

475 analysis of the effects of habitat loss and fragmentation on genetic diversity in

476 mammals. Mamm. Biol. *94*, 69–76.

477 27. Pereira, H.M., and Daily, G.C. (2006). Modeling biodiversity dynamics in countryside

478 landscapes. Ecology *87*, 1877–1885.

479 28. Koh, L.P., and Ghazoul, J. (2010). A matrix-calibrated species-area model for

480 predicting biodiversity losses due to land-use change. Conserv. Biol. *24*, 994–1001.

481 29. Marques, A., Martins, I.S., Kastner, T., Plutzar, C., Theurl, M.C., Eisenmenger, N.,

482 Huijbregts, M.A.J., Wood, R., Stadler, K., Bruckner, M., et al. (2019). Increasing

483 impacts of land use on biodiversity and carbon sequestration driven by population and

484 economic growth. Nat. Ecol. Evol. *3*, 628–637.

485 30. Garcia-Ulloa, J., Giam, X., Rondinini, C., Saura, S., and Koh, L.P. (2016).

486 Incorporating graph theory into species-area modelling of land use change impacts. In

487 the doctoral thesis of John Garcia-Ulloa: Improving Conservation Perspectives of

488 Land-Use Change Policies in the Tropics (Department of Environmental Systems

489 Science, ETH Zürich), pp. 19–47.

490 31. Saura, S., Estreguil, C., Mouton, C., and Rodríguez-Freire, M. (2011). Network

491 analysis to assess landscape connectivity trends: Application to European forests

492 (1990-2000). Ecol. Indic. *11*, 407–416.

493 32. Saura, S., and Pascual-Hortal, L. (2007). A new habitat availability index to integrate

494   connectivity in landscape conservation planning: Comparison with existing indices and

495   application to a case study. Landsc. Urban Plan. *83*, 91–103.

496   33. Fahrig, L., Arroyo-Rodríguez, V., Bennett, J.R., Boucher-Lalonde, V., Cazetta, E.,

497   Currie, D.J., Eigenbrod, F., Ford, A.T., Harrison, S.P., Watling, J.I., et al. (2019). Is

498   habitat fragmentation bad for biodiversity? Biol. Conserv. *230*, 179–186.

499   34. Fletcher, R.J., Didham, R.K., Banks-Leite, C., Barlow, J., Ewers, R.M., Rosindell, J.,

500   Holt, R.D., Gonzalez, A., Pardini, R., Damschen, E.I., et al. (2018). Is habitat

501   fragmentation good for biodiversity? Biol. Conserv. *226*, 9–15.

502   35. Betts, M.G., Wolf, C., Pfeifer, M., Banks-Leite, C., Arroyo-Rodríguez, V., Ribeiro, D.B.,

503   Barlow, J., Eigenbrod, F., Faria, D., Fletcher Jr., R.J., et al. (2019). Extinction filters

504   mediate the global effects of habitat fragmentation on animals. Science (80-.). *366*,

505   1236–1239.

506   36. Ocampo-Peñuela, Garcia-ulloa, J., Kornecki, I., Philipson, C.D., and Ghaozoul, J.

507   (2020). Impacts of four decades of forest loss on vertebrate functional habitat on

508   Borneo. Front. For. Glob. Chang. *3*, 1–13.

509   37. Wearn, O.R., Reuman, D.C., and Ewers, R.M. (2012). Extinction debt and windows of

510   conservation opportunity in the Brazilian Amazon. Science (80-.). *337*, 228–233.

511   38. Di Marco, M., Harwood, T.D., Hoskins, A.J., Ware, C., Hill, S.L.L., and Ferrier, S.

512   (2019). Projecting impacts of global climate and land-use scenarios on plant

513   biodiversity using compositional-turnover modelling. Glob. Chang. Biol. *25*, 2763–

514   2778.

515   39. Cosgrove, A.J., McWhorter, T.J., and Maron, M. (2018). Consequences of

516   impediments to animal movements at different scales: A conceptual framework and

517   review. Divers. Distrib. *24*, 448–459.

518   40. Mokany, K., Ferrier, S., Harwood, T.D., Ware, C., Di Marco, M., Grantham, H.S.,

519   Venter, O., Hoskins, A.J., and Watson, J.E.M. (2020). Reconciling global priorities for

520   conserving biodiversity habitat. Proc. Natl. Acad. Sci. U. S. A. *117*, 9906–9911.

521   41. Lindenmayer, D. (2019). Small patches make critical contributions to biodiversity

522   conservation. Proc. Natl. Acad. Sci. U. S. A. *116*, 717–719.

523   42. Pouzols, F.M., Toivonen, T., Minin, E. Di, Kukkala, A.S., Kullberg, P., Kuustera, J.,

524   Lehtomaki, J., Tenkanen, H., Verburg, P.H., and Moilanen, A. (2014). Global protected

525   area expansion is compromised by projected land-use and parochialism. Nature *516*,

526   383–386.

527   43.   Pimm, S.L., Jenkins, C.N., and Li, B. V. (2018). How to protect half of earth to ensure

528   it protects sufficient biodiversity. Sci. Adv. *4*, 1–9.

529   44.   Kok, M., Meijer, J.R., Zeist, W.-J. van, Hilbers, J., Immovilli, M., Janse, J., Stehfest, E.,

530   Bakkenes, M., Tabeau, A., Schipper, A., et al. (2020). Assessing ambitious nature

531   conservation strategies within a 2 degree warmer and food-secure world. bioRxiv,

532   2020.08.04.236489.

533   45.   Phalan, B., Onial, M., Balmford, A., and Green, R.E. (2011). Reconciling food

534   production and biodiversity conservation: land sharing and land sparing compared.

535   Science (80-.). *333*, 1289–1291.

536   46.   Püttker, T., Bueno, A.A., dos Santos de Barros, C., Sommer, S., and Pardini, R.

537   (2013). Habitat specialization interacts with habitat amount to determine dispersal

538   success of rodents in fragmented landscapes. J. Mammal. *94*, 714–726.

539   47.   Estavillo, C., Pardini, R., and Da Rocha, P.L.B. (2013). Forest loss and the biodiversity

540   threshold: An evaluation considering species habitat requirements and the use of

541   matrix habitats. PLoS One *8*, 1–10.

542   48.   McGill, B.J., Dornelas, M., Gotelli, N.J., and Magurran, A.E. (2015). Fifteen forms of

543   biodiversity trend in the anthropocene. Trends Ecol. Evol. *30*, 104–113.

544   49.   Moilanen, A. (2004). SPOMSIM: Software for stochastic patch occupancy models of

545   metapopulation dynamics. Ecol. Modell. *179*, 533–550.

546   50.   Olson, D.M., Dinerstein, E., Wikramanayake, E.D., Burgess, N.D., Powell, G.V.N.,

547   Underwood, E.C., D'amico, J. a., Itoua, I., Strand, H.E., Morrison, J.C., et al. (2001).

548   Terrestrial Ecoregions of the World: A New Map of Life on Earth. Bioscience *51*, 933–

549   938.

550   51.   Alkemade, R., Reid, R.S., van den Berg, M., de Leeuw, J., and Jeuken, M. (2013).

551   Assessing the impacts of livestock production on biodiversity in rangeland

552   ecosystems. Proc. Natl. Acad. Sci. *110*, 20900–20905.

553   52.   Gallego-Zamorano, J., Benítez-López, A., Santini, L., Hilbers, J.P., Huijbregts, M.A.J.,

554   and Schipper, A.M. (2020). Combined effects of land use and hunting on distributions

555   of tropical mammals. Conserv. Biol., 1–10.

556   53.   Burgin, C.J., Colella, J.P., Kahn, P.L., and Upham, N.S. (2018). How many species of

557   mammals are there? J. Mammal. *99*, 1–14.

558   54.   Hanski, I., and Ovaskainen, O. (2000). The metapopulation capacity of a fragmented

559   landscape. Nature *404*, 755–758.

560   55.   Bowman, J., Jaeger, J.A.G., and Fahrig, L. (2002). Dispersal distance of mammals is

561   proportional to home range size. Ecology *83*, 2049–2055.

562   56.   Hilbers, J.P., Schipper, A.M., Hendriks, A.J., Verones, F., Pereira, H.M., and

563   Huijbregts, M.A.J. (2016). An allometric approach to quantify the extinction

564   vulnerability of birds and mammals. Ecology *97*, 615–626.

565   57.   Wilman, H., Belmaker, J., Simpson, J., de la Rosa, C., Rivadeneira, M.M., and Jetz,

566   W. (2014). EltonTraits 1.0: Species-level foraging attributes of the world's birds and

567   mammals. Ecology *95*, 2027.

568   58.   Pereira, H.M., Ziv, G., and Miranda, M. (2014). Countryside species-area relationship

569   as a valid alternative to the matrix-calibrated species-area model. Conserv. Biol. *28*,

570   874–876.

571   59.   Chaudhary, A., and Brooks, T.M. (2018). Land Use Intensity-specific Global

572   Characterization Factors to Assess Product Biodiversity Footprints. Environ. Sci.

573   Technol. *52*, 5094–5104.

574

575   **Figure titles and legends**

576   **Figure 1.** Combined threats from habitat loss and fragmentation to mammal species richness

577   per ecoregion. A) Number of species committed to extinction. B) Proportion of species

578   committed to extinction. Grey = no data. Boxplots indicate the minimum, first quartile, median,

579   third quartile, and maximum of (relative) species loss values per realm. AA = Australasia (83

580   ecoregions), AN = Antarctic (2 ecoregions), AT = Afrotropic (108 ecoregions), IM = Indomalay

581   (106 ecoregions), NA = Nearctic (117 ecoregions), NT = Neotropic (172 ecoregions), OC =

582   Oceania (22 ecoregions), PA = Palearctic (197 ecoregions).
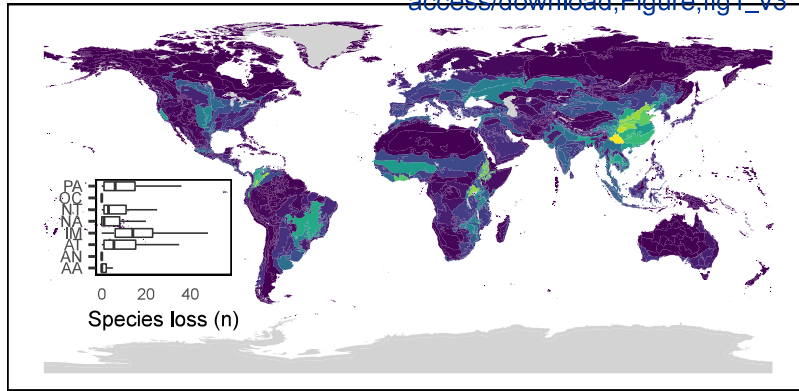
583   **Figure 2.** Predicted mammal species losses per ecoregion. Predicted losses due to A) habitat

584   conversion and B) fragmentation (ecoregions ordered by impact in the bar chart) as well as C)

585   the relative contribution of fragmentation effects to species loss (ecoregions ordered by

586   relative share of habitat conversion effects in bar chart). Grey signifies no data or zero

587   predicted extinctions (in panel C). Note the different colour scales in panels A, B, and C.

588   **Figure 3**. Relationship between predicted habitat fragmentation and habitat loss effects and

589   corresponding Spearman's rank correlation coefficient (ρ). The direction of the relationship is

590   assessed by a linear trend line (grey solid line with 95% confidence interval). The line of

591   equality (dashed) indicates that habitat conversion effects are dominant over the effects of

592   habitat fragmentation.

593   **Figure 4.** SHR predicted species loss compared with the IUCN documented number of

594   extinct and endangered species threatened by land use per ecoregion. The axis scales have

595   been square root-transformed. The plot includes the line of equality (dashed) and the linear

596   trend line (grey solid line including 95% confidence interval). The Spearman's rank correlation

597   coefficient (ρ) describes the correlation of the predicted species loss and the number of

598   extinct and endangered species as documented by the IUCN. Species with IUCN Red List

599   category 'VU', 'EN', 'CR', 'EW', and 'EX' were considered threatened or extinct. Note that

600   observations (ecoregions) may overlap, represented by a darker shade of grey.

Figure 1

A

Species loss (number of species, n)

B

Relative species loss (proportion of species, −)

Figure 2

A

Species loss (n)

Species loss (n)

Ecoregion

■ Fragmentation effects

■ Habitat conversion effects

B

Species loss (n)

Species loss (n)

Ecoregion

C

Relative contribution of fragmentation effects (−)

Contribution to species loss (−)

Ecoregion

Figure 3

Figure 4

ρ = 0.49

Predicted species loss

Documented extinct and
endangered species (IUCN)
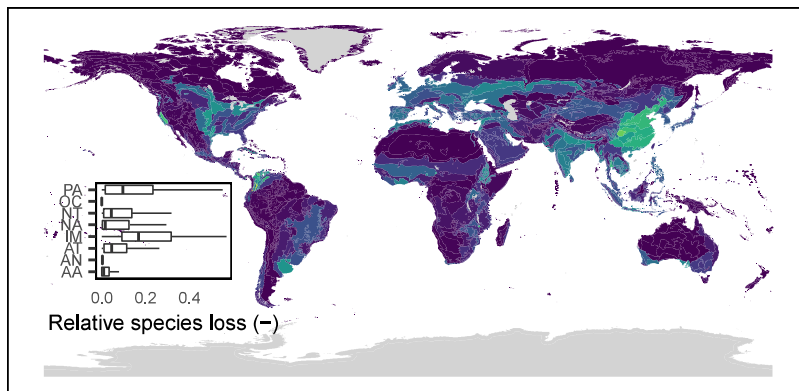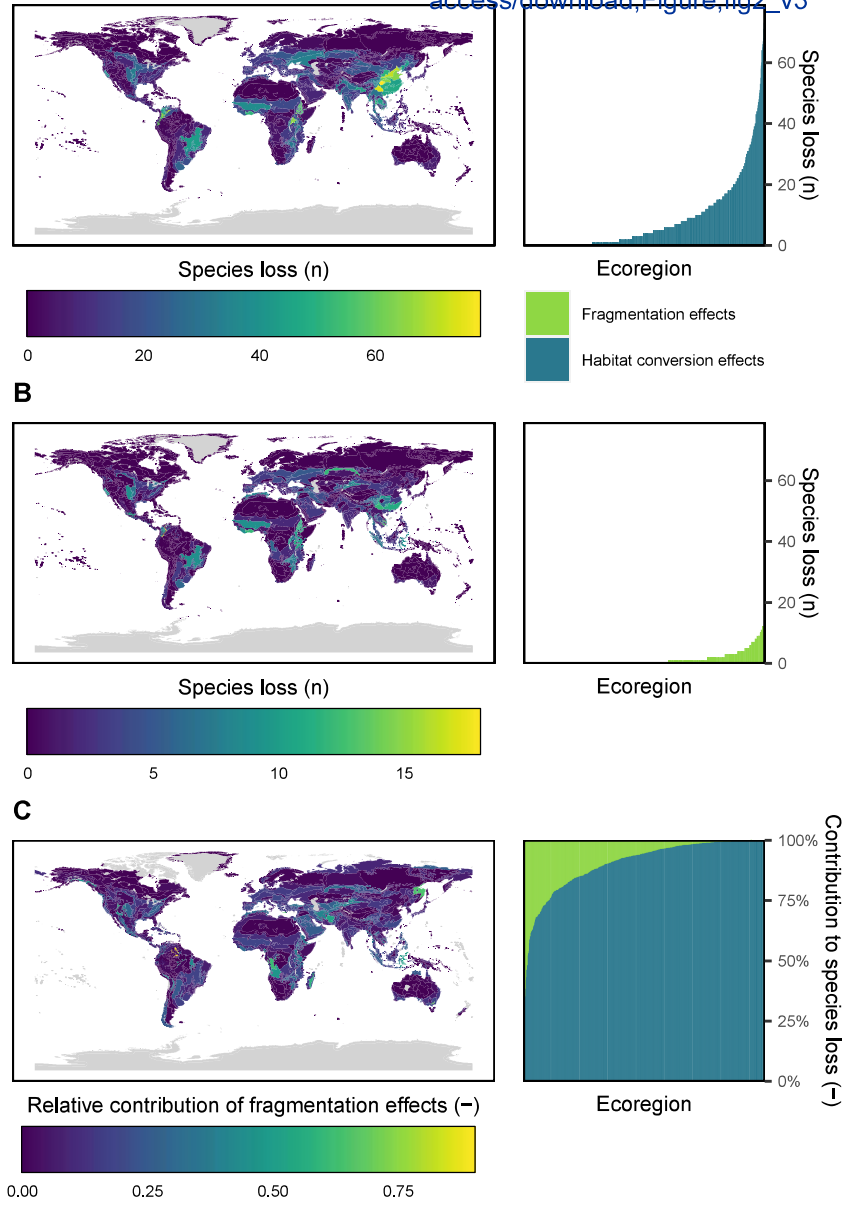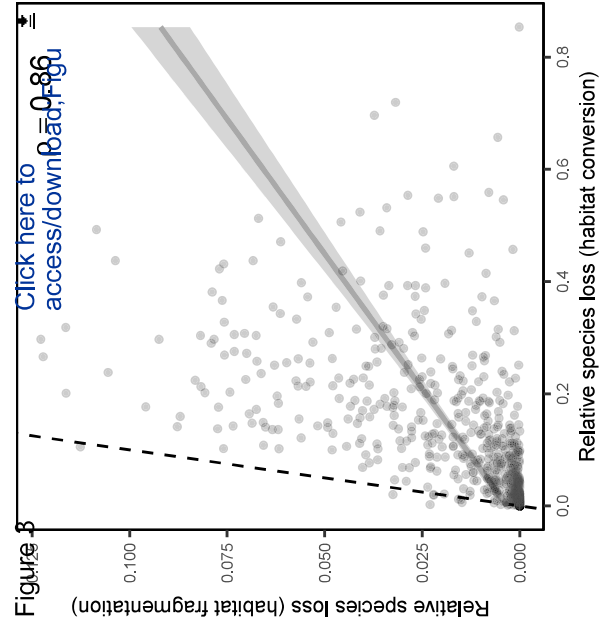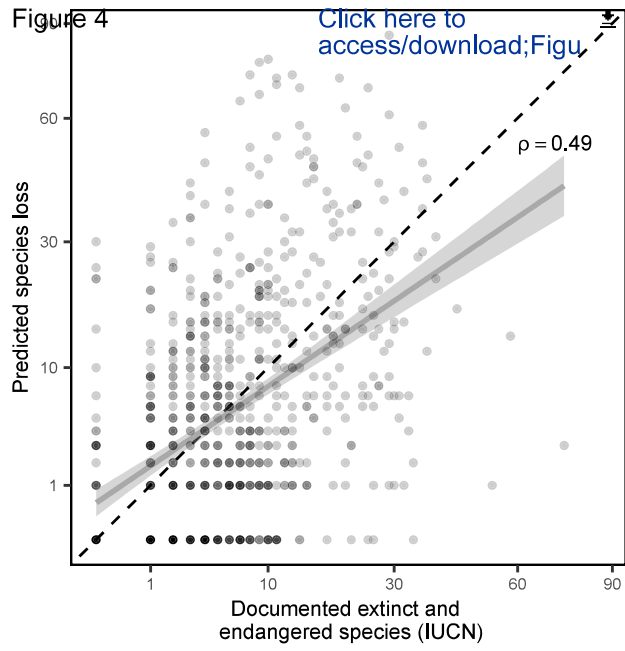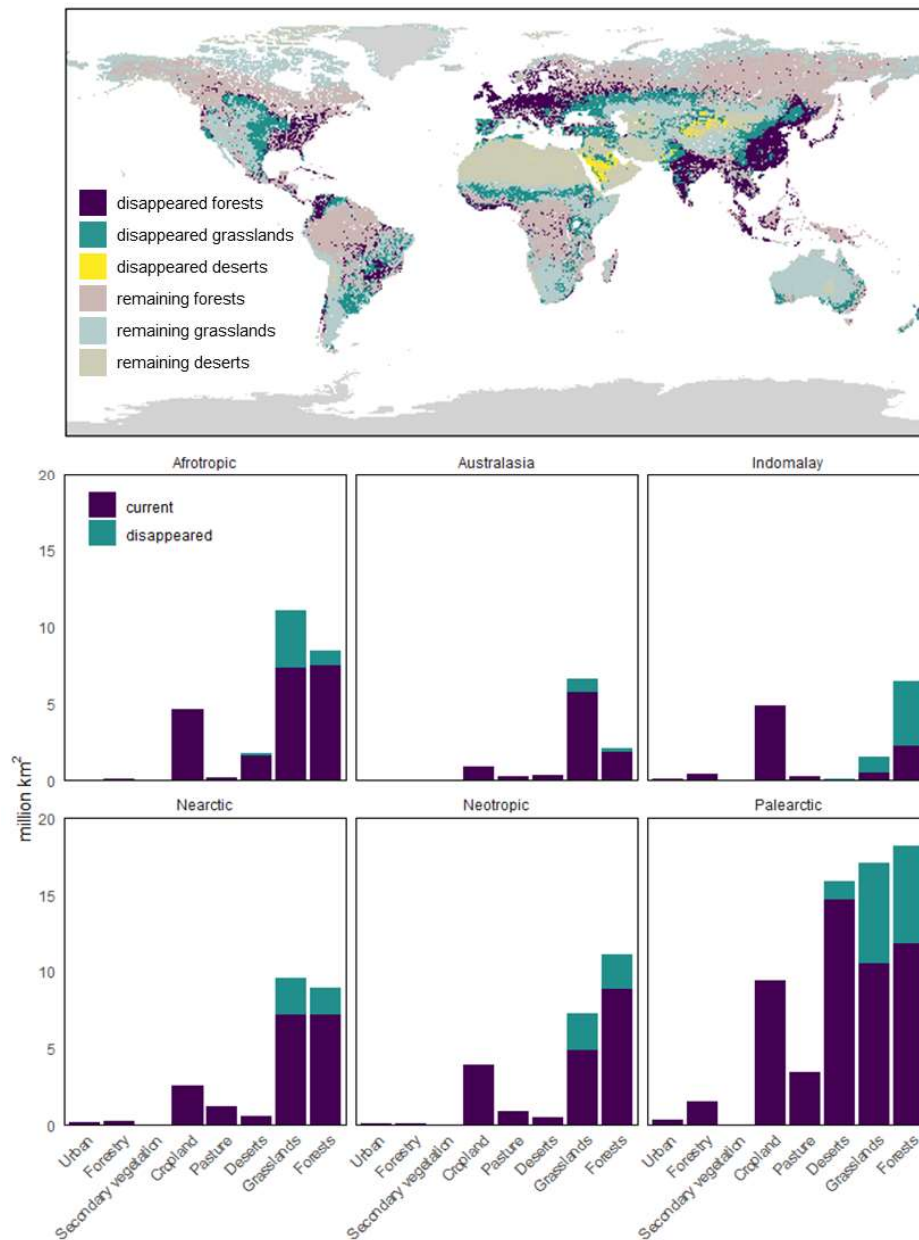
Supplemental figures

Figure S1. Global land use and land cover change. Global land use and land cover change (grey signifies no data) relative to a natural baseline based on the GLOBIO4 2015 land use map (1) and ISLSCP II Potential Natural Vegetation map (2). The predicted species losses correspond to global declines of 30% and 34% in natural forest and grassland area, respectively, relative to a natural baseline. Further, the effectively connected forest and grassland area has declined by 33% and 37%, respectively, indicating that the remaining forests and grasslands have become increasingly fragmented. This is illustrated by the increase in number of forest fragments from 0.74 million to 0.99 million, decrease in mean patch size from 75 km^2 to 39 km^2, and an increase of the mean regional inter-patch distance from 21 km to 29 km. Global grasslands fragments show a similar pattern.
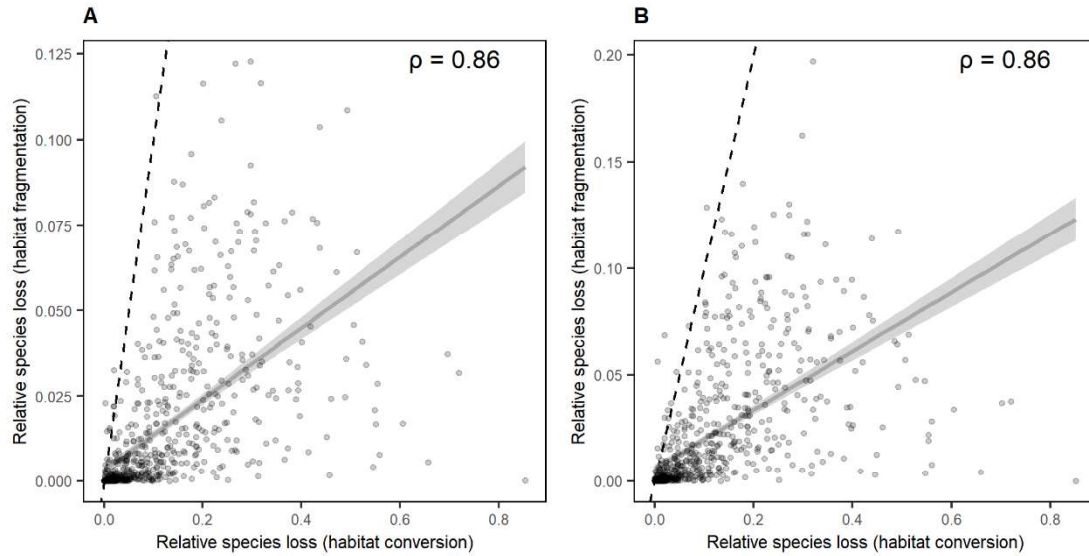
Figure S2. Predicted habitat conversion and habitat fragmentation threats per ecoregion for median and maximum natal dispersal distances. Effects based on A) maximum natal dispersal distances and B) median natal dispersal distances. The relationship between habitat conversion and fragmentation effects is assessed by the Spearman's correlation coefficient (ρ) and the direction of the relationship is indicated by a generalised linear model (grey line) with a 95% confidence interval. The identity line (dashed) indicates that habitat conversion effects are dominant over the effects of habitat fragmentation.
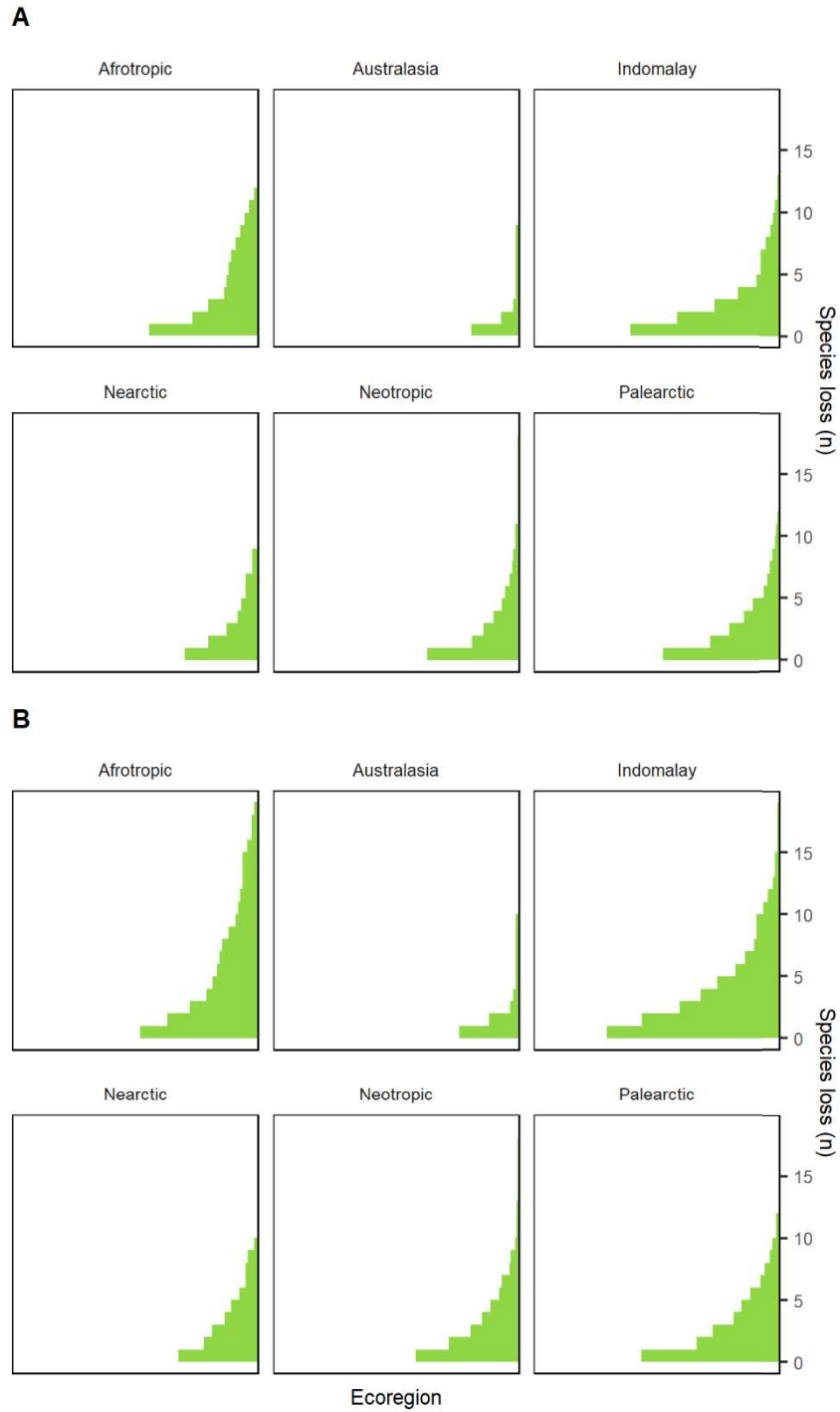
A

B

Figure S3. Predicted species loss caused by habitat fragmentation. Predicted species loss based on A) maximum natal dispersal distances and B) median natal dispersal distances. The ecoregions are grouped by realm and ordered based on the predicted fragmentation impact. Antarctic and Oceanic ecoregions are excluded because of the absence of fragmentation impacts on absolute species loss.
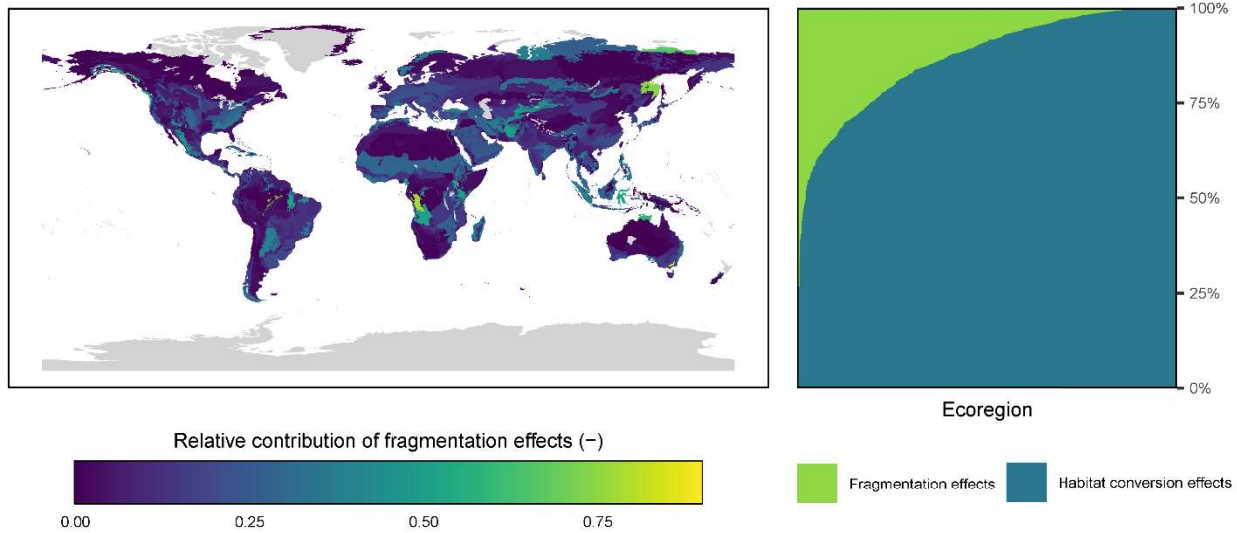
Figure S4. Relative contribution of fragmentation threats to predicted species loss based on median natal dispersal distances. Grey signifies no data or zero predicted extinctions.
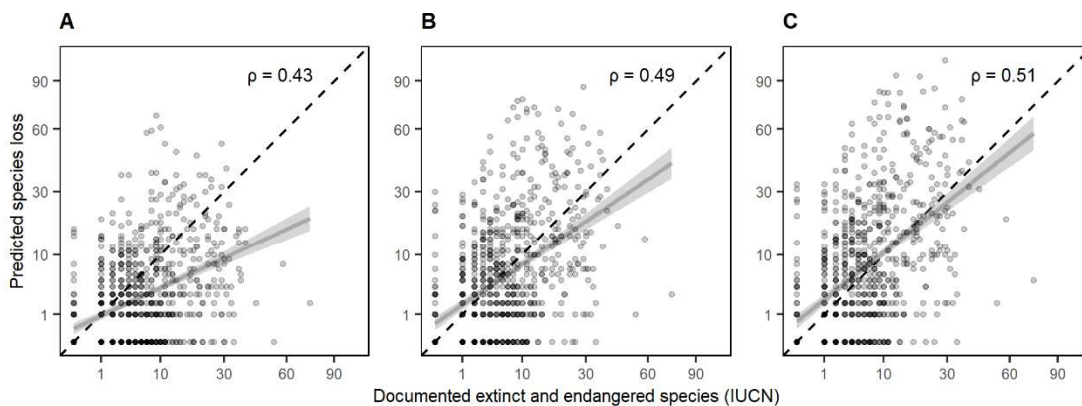

Figure S5. Predicted species loss per ecoregion according to the SHR, assuming A) minimum species accumulation rates (lower 90% confidence interval of z-value), B) a mean species accumulation rate, and C) maximum species accumulation rates (upper 90% confidence interval of z-value) compared with the documented number of extinct and endangered ('VU', 'EN', 'CR', 'EW', 'EX') species threatened by land use according to IUCN [1]. The axis scales have been square root-transformed. The line of equality is shown dashed, and the trend line is shown in grey (including 95% confidence intervals). The Spearman's rank correlation coefficient (ρ) describes the correlation of the predicted species loss and IUCN documentation on extinct and endangered species.

Supplemental tables

Table S1. Regional slopes (*z* values) of the SHR curves. Slopes for the ecoregions within each biome of the species-habitat relationship, derived from Kehoe et al. [2]. The global *z* value reported by Kehoe et al. [2] is 0.22.

Biome	SHR slope (*z*)	Lower 90% CI	Upper 90% CI
Tropical & subtropical moist broadleaf forests	0.17	0.09	0.25
Tropical & subtropical dry broadleaf forests	0.26	0.08	0.44
Tropical & subtropical coniferous forests	0.49	0.00	1.00
Temperate broadleaf & mixed forests	0.20	0.12	0.28
Temperate conifer forests	0.20	0.10	0.30
Boreal forests/taiga	0.14	0.07	0.21
Tropical & subtropical grasslands, savannas & shrublands	0.21	0.13	0.29
Temperate grasslands, savannas & shrublands	0.20	0.07	0.33
Flooded grasslands & savannas	0.23	0.00	0.46
Montane grasslands & shrublands	0.27	0.11	0.43
Tundra	0.21	0.11	0.31
Mediterranean forests, woodlands & scrub	0.26	0.11	0.41
Deserts & xeric shrublands	0.21	0.13	0.29
Mangroves	0.23	0.02	0.44

Table S2. Mean and maximum predicted regional species loss (and relative contribution of fragmentation effects to species loss) in the three different z-value scenarios (lower 90% confidence interval, mean, and upper 90% confidence interval.

Measure	Lower 90% CI	Mean CI	Upper 90% CI
Mean absolute species loss	5	10	13
Maximum absolute species loss	68	86	105
Mean relative species loss	6%	11%	14%
Maximum relative species loss	86%	85%	85%
Mean relative contribution of fragmentation effects	10%	9%	9%
Maximum relative contribution of fragmentation effects	90%	90%	90%

Table S3. Predicted regional species loss (and relative contribution of fragmentation effects to species loss) in selected ecoregions using three land cover resolutions (300 m, 1 km, and 3 km).

Realm	Region (ID)	Area (km²)	Species loss (relative loss)			Contribution of fragmentation effects		
			300 m	1 km	3 km	300 m	1 km	3 km
Afrotropic	Mandara Plateau mosaic (30710)	7479	33 (48%)	35 (51%)	37 (55%)	6%	5%	3%
Indomalay	Sumatran tropical pine forests (40304)	2748	7 (7%)	7 (7%)	7 (7%)	10%	9%	1%
Neotropic	Tehuacán Valley matorral (61316)	9862	17 (17%)	17 (18%)	17 (18%)	16%	14%	12%
Nearctic	Florida sand pine scrub (50513)	3879	5 (12%)	5 (12%)	5 (13%)	1%	1%	1%

Table S4. Land type aggregation of the GLOBIO4 [3] land use and ISLSCP PNV [4] land cover maps.

ID	land type	GLOBIO ID	GLOBIO4 land type	PNV ID	PNV land cover type
0	No data	0	No data	16	No data
1	Urban	1	Urban		
2	Cropland	230	Cropland, light use		
		231	Cropland, intense use		
3	Pasture	3	Pasture, intense use		
		4	Pasture, light use*		
4	Forestry	5	Forestry		
11	Forests	50	Tree cover, broadleaved, evergreen, closed to open (>15%)	1	Tropical evergreen forest
		60	Tree cover, broadleaved, deciduous, closed to open (>15%)	2	Tropical deciduous forest
		61	Tree cover, broadleaved, deciduous closed (>40%)	3	Temperate broadleaf evergreen forest
		62	Tree cover, broadleaved, deciduous, open (15-40%)	4	Temperate needleleaf evergreen forest
		70	Tree cover, needle leaved, evergreen, closed to open (>15%)	5	Temperate deciduous forest
		71	Tree cover, needle-leaved, evergreen, closed (>40%)	6	Boreal evergreen forest
		72	Tree cover, needle-leaved, evergreen open (15-40%)	7	Boreal deciduous forest
		80	Tree cover, needle -leaved, deciduous, closed to open (>15%)	8	Mixed forest
		81	Tree cover, needle-leaved, deciduous, closed (>40%)		
		82	Tree cover, needle-leaved, decidu1ous, open (15-40%)		
		90	Tree cover, mixed leaf type (broadleaved and needle-leaved)		
		100	Mosaic tree and shrub (>50%) / herbaceous cover (<50%)		
		160	Tree cover, flooded, fresh or brackish water		
		170	Tree cover, flooded, saline water		
12	Grasslands	110	Montane Grasslands and Shrublands [agg]; Mosaic tree and shrub (>50%) / herbaceous cover (<50%) [crop]	9	Savanna
		120	Shrubland	10	Grassland/steppe
		121	Evergreen shrubland	11	Dense shrubland
		122	Deciduous shrubland	12	Open shrubland
		130	Grassland	13	Tundra
		140	Lichens and mosses		
		150	Sparse vegetation (tree, shrub, herbaceous cover) (<15%)		
		151	Sparse tree cover (<15%)		
		152	Sparse shrub (<15%)		
		153	Sparse herbaceous cover (<15%)		
		180	Shrub or herbaceous cover, flooded, fresh/saline/brackish water		
13	Deserts	200	Bare areas	14	Desert
		202	Unconsolidated bare areas		
15	Water bodies	210	Water bodies	0	Water bodies
16	Rock & ice	201	Consolidated bare areas	15	Polar desert/rock & ice
		220	Permanent snow and ice		

* The GLOBIO4 "Pasture, light use" class was replaced by the original ESA European Space Agency Climate Change Initiative landcover [5], resulting in replacement by one of the natural landcover types (GLOBIO4 ID 50-180, 199-220).

Supplemental references

1. IUCN (2020). The IUCN Red List of Threatened Species. Version 2020-2. http://www.iucnredlist.org.
2. Kehoe, L., Senf, C., Meyer, C., Gerstner, K., Kreft, H., and Kuemmerle, T. (2017). Agriculture rivals biomes in predicting global species richness. Ecography (Cop.). *40*, 1118–1128.
3. Schipper, A.M., Hilbers, J.P., Meijer, J., Antão, J., Benítez-López, A., de Jonge, M., Leemans, L., Scheper, E., Alkemade, R., Doelman, J., et al. (2020). Projecting terrestrial biodiversity intactness with GLOBIO 4. Glob. Chang. Biol. *26*, 760–771.
4. Ramankutty, N., Foley, J.A., Hall, F., Gollatz, G., Meeson, B., Los, S., Brown de Colstoun, E., and Landis, D. (2010). ISLSCP II Potential Natural Vegetation cover.
5. ESA (2017). Land Cover CCI Product, User Guide Version 2.0. 1–104. http://maps.elie.ucl.ac.be/CCI/viewer/download/ESACCI-LC-Ph2-PUGv2_2.0.pdf.